e-Prime - Advances in Electrical Engineering, Electronics and Energy 2 (2022) 100064

Contents lists available at ScienceDirect

e-Prime - Advances in Electrical Engineering, Electronics and Energy

journal homepage: www.elsevier.com/locate/prime

# Thermoeconomic and exergoenvironmental sustainability of a power-cooling organic Rankine cycle with ejector system

Fidelis I. Abam [a,b,*], Bassey B. Okon [c], Ekwe B Ekwe [a], John Isaac [a], Samuel O Effiom [d], Macmanus C Ndukwu [e], Oliver I. Inah [f], Paschal A Ubi [f], Sunday Oyedepo [g], Olayinka S Ohunakin [g]

[a] Department of Mechanical Engineering, Energy, Exergy and Environment Research Group (EEERG), Michael Okpara University of Agriculture, Umudike, P.M.B., Umuahia 7267, Nigeria
[b] Africa Centre of Excellence for Sustainable Power and Energy Development, University of Nigeria Nsukka, Nigeria
[c] Department of Mechanical Engineering, Akwa Ibom State University Ikot-Akpaden, Nigeria
[d] Department of Mechanical Engineering, Cross River University of Technology, Calabar, Nigeria
[e] Department of Agricultural and Bioresources Engineering, Michael Okpara University of Agriculture Umudike, P.M.B., Umuahia 7267, Nigeria
[f] Department of Mechanical Engineering, University of Calabar, Calabar, Nigeria
[g] Department of Mechanical Engineering, Covenant University Ota, Nigeria

ARTICLE INFO

*Keywords:*
Exergoenvironmental
Turbine
Refrigerants
Energy
Life-cycle

ABSTRACT

The study presents a power-cooling organic Rankine cycle with an ejector system (ORCPCES). The objective is to determine the thermodynamic, economic and sustainability of the ORCPCES from the manufacturing, commissioning and decommissioning phases. Component-wise modelling was first performed based on the exergy concept. The system simulation was carried out using a developed source code in Engineering Equation Solver (EES). The refrigerant leakages and the material component impact on the environment were evaluated at all phases of the plant life cycle. The results indicate that the evaporator cooling rate (ECR) and the power-cooling efficiency (PCE) varied from 120.8 to 153 kW and 28.87 to 34.43 % across the refrigerants with the highest PCE and exergy efficiency obtained using R1234ze. The maximum power output was obtained using R1234ze. The overall environmental impact due to the components occurred at $5.1 \times 10^5$ mPts, $5.24 \times 10^5$ mPts and $5.4 \times 10^5$ mPts for R245fa, R1234yf, and R1234ze, respectively, while $4.01 \times 10^5$ mPts $7.81 \times 10^4$ mPts and $9.33 \times 10^5$ mPts was due to the working fluids in that order. The unit cost of electricity (UCOE) across the refrigerants varies from 0.181$/kWh to 0.2291$/kWh with the least UCOE, 0.181$/kWh obtained using R1234ze. The highest exergetic sustainability index of 0.56 was achieved using R1234ze.

## 1. Introduction

Energy is indispensable for the sustainability of life, and its cautious utilization is progressively acknowledged as playing an essential role in the various engineering and environmental processes. Recovering and utilizing the low waste heat from power generating plants and industrial waste, and using renewable fuels, remains an impelling and promising approach to sustainably resolving global energy-related concerns [1,2]. Many low heat temperature cycles exist for waste heat utilization. Such include the supercritical Rankine cycle (SRC), organic Rankine cycle (ORC), trilateral flash cycle, Goswami cycle and Kalina cycle [3,4]. The ORC has recently attracted wide attention and interest due to its low maintenance cost, simplicity in application, low-pressure requirement, and high recovering efficiency [5,6]. In the industry today, the cooling need has increased significantly due to the advancement and growing demand in many industrial applications. However, to increase the power production capacity and total efficiency of applicable systems and supply a concurrent cooling capacity, a number of integrated ORC power-cooling refrigerating cycles with ejector systems have been proposed.

Furthermore, many researchers have presented studies on ORC-based power cooling cycles with ejector systems. For example, Rostamzadeh et al. [7] presented the performance of a basic combined power-cooling ejector system (BCCP) and adapted three combined cycle plants (CCP). The adapted CCP cycles are integrated with a suitable

* Corresponding author.
*E-mail address:* abamfidelis@mouau.edu.ng (F.I. Abam).

https://doi.org/10.1016/j.prime.2022.100064
Received 19 April 2022; Received in revised form 4 August 2022; Accepted 8 September 2022
Available online 9 September 2022

**Nomenclature**

| | |
|---|---|
| BEP | break-even point |
| $\dot{E}$ | exergy flow rate (kW) |
| ECR | evaporator cooling rate (kW) |
| EDR | exergy destruction ratio |
| EEF | environmental effect factor |
| EES | engineering equation solver |
| ESI | exergetic sustainability index |
| Fb | exergoenvironmental parameter |
| h | specific enthalpy (kJ/kg) |
| LCC | life cycle cost ($) |
| $\dot{m}$ | mass flow rate (kg/s) |
| ORC | organic Rankine cycle |
| ORCPCES | organic Rankine cycle power-cooling ejector system |
| P | pressure (kPa) |
| PCE | power-cooling efficiency (%) |
| $\dot{Q}$ | heat input rate (kW) |
| rb | relative difference |
| T | temperature (K) |
| V | velocity (m/s) |
| $\dot{W}$ | work input rate (kW) |
| WER | waste exergy ratio |
| $\dot{Y}$ | exergoenvironmental impact (mPts) |
| Z | Purchase equipment cost ($) |

*Greek symbols*

| | |
|---|---|
| $\eta$ | efficiency |
| $\psi$ | exergy efficiency |
| $\omega$ | entrainment ratio |

*Subscripts*

| | |
|---|---|
| D | destruction |
| d | diffuser |
| e | exit |
| F | fuel |
| i | inlet |
| L | loss |
| k | component |
| pf | primary flow |
| zn | nozzle |

combination of the ORC ejector cooling (refrigeration) cycles (ERC) to produce power and cooling concurrently. The working fluids considered were R123, R245fa and Isobutane as a fixed fluid. The study indicates that the thermal efficiency, overall exergy destruction ratio and exergy efficiency can be improved by 24.5, 32 and 72 %, respectively. From the environmental viewpoint, selecting R123/Isobutane working fluids for the combined system incorporated with turbine bleeding and recuperation was most appropriate. The study of Kheiri et al. [8] considered four different configurations of an ORC system: ORC integrated with ejector (EORC), ORC combined with regenerator (ERORC), ORC integrated with ejector, feed fluid heater (EFFHORC) and ORC integrate with ejector, feed fluid heater and regenerator (ERFFHORC). The results show that Cis2-Butene and R245fa had the highest overall power output and thermal efficiency from the operational refrigerants used for all the adapted cycles. The ERFFHORC and the generic ORC operated with R245fa had the maximum and the minimum thermal efficiency. Similarly, the study obtained an improved efficiency for EORC, ERORC, EFFHORC and ERFFHORC at 13.21%, 15.30 %, 18.35 % and 19.29 %, respectively.

Additionally, the performance improvement of a generic combined power cooling cycle (CCP) was studied by Ebadollahi et al. [9] to enhance energy and exergy efficiencies. However, a cascaded ejector refrigeration system was proposed to be integrated with an ORC for power and cooling production. The system was also optimized to attain the optimum operating and cost-effective parameters. The findings show that the freezing load, energy efficiency, net electricity, exergy efficiency and unit cost of products were estimated at 35.33 kW, 48.32 %, 64.03 kW, and 404 $/GJ, respectively. Zhu et al. [10] analyzed an innovative ejector heat pump integrated with an ORC ejector system for cooling, power and heat production using zeotropic mixtures. The study compared the performance of a generic ORC, ORCs with post-ejector, ORC with ejector heat pump, and ORC with ejector. The results indicate that the ejector heat pump integrated with the ORC, combined cooling, heating and power generation was thermodynamically feasible and cost-effective. Zheng and Weng [11] investigated an integrated power ejector refrigeration system. The anticipated system combines the ORC and the ejector cooling cycle. The system simulation was performed using R245fa refrigerant. The results obtained thermal and effective efficiencies of 34.1 and 18.7 %, respectively, while the exergy efficiency was calculated at 56.8 %. The study inferred that there exists a high potential in the proposed cycle for cooling production.

Further studies include the works of Garcia and Berana [12]. They proposed an innovative combined power and cooling system where an ORC cycle is integrated with a compressor-driven ejector-refrigeration cycle. The main ejector flow for the refrigeration cycle emanates from one of the condenser streams. The proposed cycle simulation was performed using three refrigerants, R245fa, R123, and R141b. The study shows that the system COP was enhanced at increasing evaporator temperature while the exergy efficiency varies contrariwise with the entrainment ratio. The system's performance was further enhanced using R141b refrigerant and showed the highest exergy efficiency and COP of 46.23% and 3. 26, respectively. A thermodynamic parametric study on a combined ORC system with an ejector refrigeration system was performed in [13]. Four working fluids were investigated: R141b, R245fa, R600a, and R601a. The performance criteria were based on the first and second laws of thermodynamics. In this system, the fluid from the ejector after expansion and the bled fluid is mixed at some point and preheated before condensation and evaporation. The results show that R141b working fluid had the smallest optimal pressure and the smallest overall thermal conductance at the optimum conditions. Equally, the R601a refrigerant had the maximum exergy efficiency and the lowest total exergy destruction in the optimum cases

Similarly, Toujani et al. [14] developed three different configurations of ORC systems for combined power and cooling production. In addition, the developed combination of the ORC system and the vapor compression system was used for cogeneration with a negative-cold (-10 to 0 °C) and a positive-cold (0 to 10 °C). The system was examined based on energy efficiency, net power production and refrigeration capacity. The study shows that the cogeneration system with the negative cold utilisation had the highest performance. A maximum work output and cooling rate of about 65 kW and 1000 kW were achieved. The global coefficient obtained was not greater than 1.05, and the system was not only restricted to be used for temperature ranges between -10 °C and 10 °C but is also feasible with fluids with lower temperatures (congelation temperatures).

Conversely, studies have shown that the performance of ORC systems is also influenced by factors which include system design or configurations, type of working fluids and operating parameters. For example, Gu et al. [15] proposed a thermal analysis of a low-temperature ORC using R245fa as a working fluid. They inferred that R245fa with the particular ORC configuration had better efficiency. Likewise, Hajabdollahi et al. [16] provided the performance of an ORC

using different working fluids, which comprise R22, R123, R245fa and R134a. Different power outputs and efficiencies were obtained for each working fluid. The result shows that the system's performance discrepancies are attributed to the thermophysical properties of the working fluids. Other investigations are that of Hettiarachchi et al. [17], who appraised the performance of R123, PF 5050 and n-pentane refrigerants for a geothermal organic Rankine cycle. At the same time, Saleh et al. [18] examined 31 refrigerants for supercritical and sub-critical ORCs applied to a geothermal power system. Both studies arrived at the common conclusion that refrigerant type is critical to ORC performance and environmental sustainability. Abam et al. [19] considered the thermo-sustainability indicators (TSI) for different ORC configurations and working fluids. The TSIs are environmental parameters based on the second law of thermodynamics. The results show that high sustainability index of 0.65 was obtained using R245fa, while a high environmental effect factor of 1.5 was obtained using R1234ze.

Additionally, integrating the ejector refrigeration cycle into the ORC system has shown performance enhancement and the use of different working fluids. System configuration, component sizing, and choosing appropriate stream pathways to reduce the number of components are germane to lowering cost and maintaining environmental sustainability. The latter factors form the central pivot from which the objectives and contributions of this study are derived, as presented in the subsequent section.

### 1.1. Motivation and contribution of the research

From the reviewed literature, varying the ORC configurations, especially incorporating an ejector for cooling, has enhanced the ORC system products and thermal efficiency. Nonetheless, the power-cooling ORC cycles with an ejector often require an additional high-pressure pump to provide pressure for the primary ejector channel. For example, the studies in Kheiri et al. [7] and Rostamzadeh et al. [8] had multiple pumps for the adapted combined power cooling cycles. The additional pumps reduce the net system output, which can significantly impact the system's thermal efficiency. Also, in Habibzadeh et al. [13], the fluid from the ejector after expansion and that bled from the turbine are mixed at some point and preheated before condensation and evaporation. The concern about this configuration is that the additional heat to the working fluid will require a large condenser area for complete condensation. However, to close this gap, this research proposes a power-cooling ORC system where the primary ejector flow is provided by bled refrigerant from the turbine at sufficient pressure and temperature at the partial expansion of the turbine, thus, avoiding an additional pump and preheater in this regard. Secondly, the fluid after the expansion from the turbine is mixed with that from the ejector before condensation, avoiding a preheater as in Habibzadeh et al. [13] and operated at a temperature and pressure that will ensure condensation with a sizable heat rejection unit. The objective, therefore, is to propose a system for producing power and cooling with reduced components in a simple ORC configuration. The study will also develop and evaluate the cycle and component impact on the environment and working fluid sustainability from the manufacturing, commissioning and decommissioning phases, an analysis absent in the previous studies.

### 1.2. System description

Fig. 1 shows the proposed ORC power-cooling ejector system (ORCPCES). The system comprises a vapour generator, turbine, ejector, pump, throttling valve, evaporator and condenser. The waste heat powers the ORCPCES from a modular biomass-fired turbine. The waste heat is collected in the receiver tube containing the heating oil, thus increasing the temperature of the oil to its boiling point. This high-temperature fluid inside the receiver tube transfers its thermal energy to the refrigerant passing through the heat recovery vapour generator (HRVG). The super-heated refrigerant vapour at state 4 expands in the turbine to drive a coupled generator for power generation. At state 5, part of the working fluid is bled, passing through the ejector nozzle.

The very high-velocity refrigerant vapour at the exit of the nozzle creates a vacuum at the inlet of the mixing chamber. It entrains a secondary vapour from the evaporator state 12 into the ejector chamber. The stream at state 6 mixes with the stream from the turbine exhaust at state 7. It enters the condenser, where it condenses to saturated liquid. In state 8, the saturated liquid is divided into two parts (states 9 and 10). Part of the fluid passes through the throttling valve at state 9, where the temperature and pressure are reduced. The low temperature and pressure fluid evaporate in the evaporator at state 11, thus producing cooling. The other part of the fluid at state 10 is pumped to the HRVG to start the cycle.

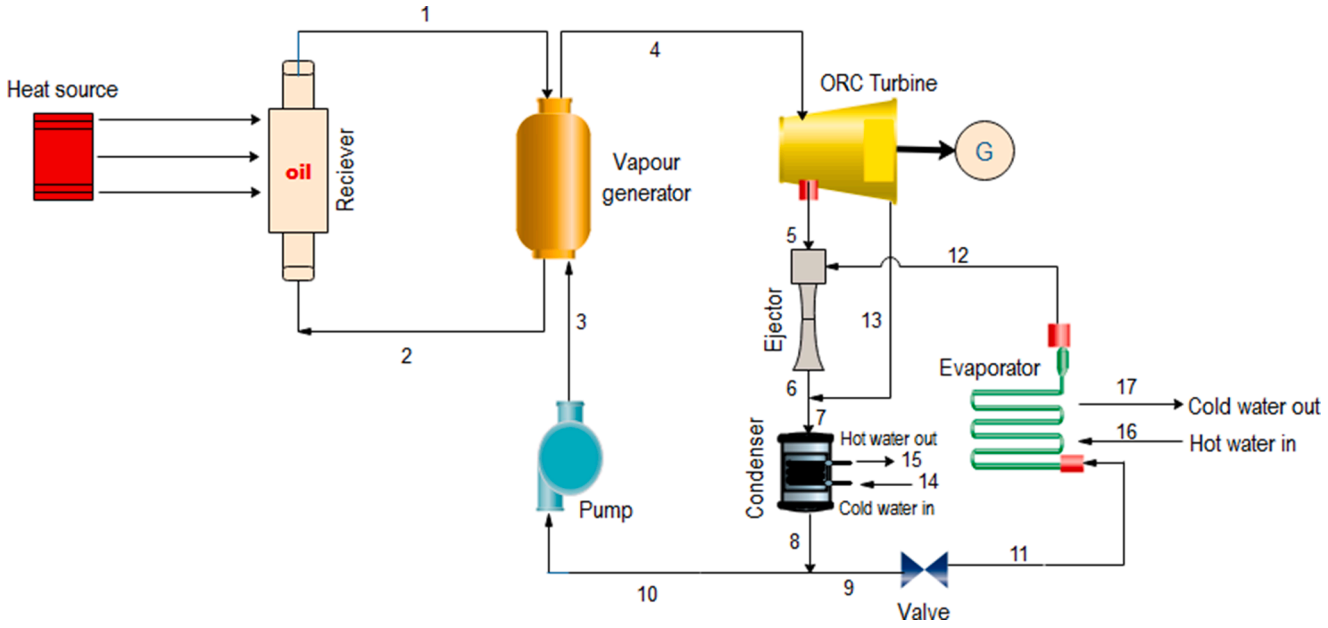


**Fig. 1.** Schematic diagram of ORC power-cooling ejector cycle (ORCPCES).

## 2. Methods and model development of the ORCPCES

### 2.1. Thermodynamic modeling of the ORCPCES

The following assumptions were considered in the analysis of the ORCPCES: (1) the fluid flow condition in the system component is steady. (2) The components' pressure, friction and heat losses are ignored. (3) The system boundaries were treated as adiabatic, so the heat losses to the surroundings were neglected. (4) The heat source is a hot exhaust stream from a modular turbine at 200 °C (473 K), with the heat source flow rate at 20 kg/s [20]. (5) The pump and turbine isentropic efficiencies were kept at 0.70 and 0.85, respectively [21]. (6) The evaporator and condenser pinch point temperature difference, and the ambient temperature are maintained at 278 K, 283 K and 293.17 K, respectively [22]. (7) The diffuser, nozzle, and ejector mixing chamber efficiencies are 0.85, 0.85 and 0.95, respectively [23]. (8) A constant pressure mixing process exists in the ejector mixing chamber. (9) The outlet pressure of the nozzle is equivalent to the inlet secondary pressure inlet, and the ejector flow velocities inlet and the outlet are insignificant. Thus, the ejector modelling data are obtained equally in [23,24].

#### 2.1.2. Energy analysis

The steady-state energy flow process involving the energy stream is presented in Eq. (1) [7, 25].

$$\sum \dot{Q}_k + \sum \dot{m}_i h_i = \sum \dot{m}_i h_0 + \sum \dot{W} \tag{1}$$

The energy and mass balances are defined for steady-state conditions, neglecting potential and kinetic energies. Eq. (1), based on the assumptions, was applied to Fig. 1 to balance the energy flow in the respective components as depicted in Appendix A1

#### 2.1.3. ORC ejector modelling

The ejector is a type of pump that uses the venturi effect of a converging-diverging nozzle to convert the mechanical energy (pressure) of a motive fluid to kinetic energy (velocity) by creating a low-pressure zone that attracts in and entrains a suction fluid. After the fluid must have passed through the section of the ejector's throat, the expansion of mixed fluid occurs with a reduction in the fluid velocity. The mixed fluids are recompressed by converting back the velocity to pressure. The drive fluid could be either gas, steam or liquid. The process occurring in the ejector is assumed to be steady-state, one-dimensional and adiabatic, and no work is done during the process. The velocities can be considered negligible at the ejector's inlet and outlet. In this study, the primary motive flow enters the ejector at point 5. The suction flow exits the evaporator at point 13. The process in the ejector includes the expansion of the high-pressure prime motive flow through the nozzle, mixing with the low-pressure secondary flow in the mixing section at constant pressure, and diffusing to the outlet of the ejector (point 6). At the same time, the kinetic energy of the mixture is converted to the pressure head. Therefore, an essential parameter for the secondary flow is the entrainment ratio, defined as:

$$\omega = \frac{\dot{m}_{12}}{\dot{m}_5} \tag{2}$$

In the nozzle section, the inlet velocity of the primary flow $V_{pf,\ n1}$ is negligible, so the exit enthalpy and velocity of primary flow and nozzle efficiency are expressed by Haghparast et al. [24] in Eqs. (3) and (4).

$$V_{pf,\ n2} = \sqrt{2\eta_{Noz}\left(h_{pf,\ n1} - h_{pf,\ n2,s}\right)} \tag{3}$$

$$\eta_{Noz} = \frac{h\dot{p}f_1\ \dot{n}_1\ -\ h\dot{p}f_1\ \dot{n}_2}{h\dot{p}f_1\ \dot{n}_1\ -\ h\dot{p}f,\dot{n}_{2,s}} \tag{4}$$

where $h_{pf,\ n1}$ is the enthalpy at point 2 and $h_{pf,\ n2,s}$ is the exit enthalpy of the primary flow under isentropic expansion and $\eta_{Noz}$ is the nozzle efficiency. The momentum conservation equation for the mixing chamber area gives the following relationship:

$$\dot{m}_5 V_{pf,\ n2} + \dot{m}_{12} V_{sf,\ n2} = (\dot{m}_5 + \dot{m}_{12}) V_{mf,\ m,s} \tag{5}$$

Neglecting the secondary flow velocity $V_{sf,\ n2}$ compared to the primary flow velocity $V_{pf,\ n2}$.The exit velocity of mixed flow $V_{mf,\ m,s}$ can be expressed as:

$$V_{mf,\ m,s} = \frac{V_{pf,\ n2}}{1+\omega} \tag{6}$$

The mixing chamber efficiency can be expressed as

$$\eta_{Mix} = \frac{V^2_{mf,m}}{V^2_{mf,ms}} \tag{7}$$

Therefore, the actual velocity of the mixed flow is expressed as:

$$V_{mf,\ m,s} = \frac{V_{pf,\ n2}\sqrt{\eta_{Mix}}}{V^2_{mf,ms}} \tag{8}$$

The energy equation for the mixing chamber gives:

$$\dot{m}_5\left(h_{pf,\ n2} + \frac{V^2_{pf,n_2}}{2}\right) + \dot{m}_{12}\left(h_{sf,\ n_2} + \frac{V^2_{sf,n_2}}{2}\right) = \dot{m}_6\left(h_{mf,m} + \frac{V^2_{mf,\ m}}{2}\right) \tag{9}$$

By simplifying Eqs (8) and (9), the enthalpy of mixed flow is obtained:

$$h_{mf,m} = \frac{h_{pf,\ n_1} + \omega h_{sf,\ n_2}}{1+\omega} - \frac{V^2_{mf,\ m}}{2} \tag{10}$$

The mixed flow converts its kinetic energy to a pressure increase in the diffuser section. Assuming the exit velocity of the mixed flow to be negligible and considering the diffuser efficiency, the actual exit enthalpy of the mixed flow and the diffuser efficiency are determined:

$$h_6 = h_{mf,m} + \left(h_{mf,ds} - h_{mf,m}\right)/\eta_{Dif} \tag{11}$$

$$\eta_{Dif} = \frac{h_{mf,\ d,_s} - h_{mf,\ m}}{h_{mf,\ d} - h_{mf,\ m}} \tag{12}$$

where $h_{mf,ds}$ is the ideal exit enthalpy of the mixed flow with isentropic compression, and $\eta_{Dif}$ is the diffuser efficiency. The entrainment ratio is expressed in Eq. (13) [24].

$$\omega = \sqrt{\eta_{Noz}\eta_{Mix}\eta_{Dif}\left(\frac{h_5 - h_a}{h_{13} - h_b}\right)} - 1 \tag{13}$$

where $\eta_{Noz}$, $\eta_{Mix}$, $\eta_{Dif}$ are the nozzle efficiency, nozzle mixing chamber and diffuser efficiency.

#### 2.1.4. Exergy analysis

The general exergy balance for a system in steady-state neglecting potential, kinetic and electrical energy is defined in Ifaei [25] and Abam et al. [26] as:

$$\dot{E}_{xd} = \sum_k \left(1 - \frac{T_0}{T_k}\right)\dot{Q}_k - \dot{W}_{cv} + \sum_i (n_i \dot{E}x_i) + \sum_e (n_e \dot{E}x_e) \tag{14}$$

where $\dot{E}_{xd}$ is the exergy destruction rate, $\left(1 - \frac{T_0}{T_k}\right)\dot{Q}_k$ is the exergy flow rate accompanied by heat transfer, $\dot{W}_{cv}$ is the rate of work done within the control volume, $n_i\dot{E}x_i$ and $n_e\dot{E}x_e$ is the exergy flow rate in and out of the control volume. Additionally, the exergy destruction can be expressed in products and fuel [25, 27].

$$\dot{E}_{D,k} = \dot{E}_{F,k} - \dot{E}_{Pk-}\dot{E}_{L,k} \tag{15}$$

The exergy efficiency, $\psi_k$ and the exergy destruction and exergy loss ratio are equally defined for the k component as in Eqs. (16) to (18).

$$\psi_k = \frac{\dot{E}_{Pk}}{\dot{E}_{F,k}} = 1 - \left[\frac{\dot{E}_{D,k} + \dot{E}_{L,k}}{\dot{E}_{F,k}}\right] \tag{16}$$

$$Y_{D,k} = \frac{\dot{E}_{D,k}}{\dot{E}_{F,total}} \tag{17}$$

$$Y_{L,k} = \frac{\dot{E}_{L,k}}{\dot{E}_{F,total}} \tag{18}$$

where $\dot{E}$, D, P, L F, and k connote exergy rate, exergy destruction, product, loss, fuel and component, respectively.

The exergy destruction, exergy flow rates, and the component efficiencies for Fig. 1 are derived and depicted in Appendix A2.

#### 2.1.5. System performance criteria for the ORCPCES

The following performance indicators have been applied in determining the thermal performance of the ORCPCES [28].

*(i) The power-cooling efficiency*: the efficiency of the combined power-refrigerating system is calculated from the ratio of the aggregate output power and the overall cooling produced to the system input heat.

$$\eta_{power-cooling} = \frac{\dot{W}_{net} + \dot{Q}_{evp}}{\dot{Q}_{in}} \tag{19}$$

$$\dot{W}_{net} = \dot{W}_{tub} - \dot{W}_{pump} \tag{20}$$

*(ii) Exergy efficiency*: The exergy efficiency of the system is the ratio of the total output exergy to the total input exergy presented as,

$$\varphi = \frac{\dot{W}_{tub} + \dot{E}_{x\ \text{evap, total}}}{\dot{E}_{x,total}} \tag{21}$$

where $\dot{E}_{x,total}$(kW) is the total input exergy expressed as $\left(1 - \frac{T_0}{T_{Qin}}\right)\dot{Q}_{in}$ and $\dot{E}_{x\ evap,total}$ (kW) described the total exergy of refrigeration.

#### 2.1.6. Exergetic sustainability indicators and exergoenvironmental evaluation

Further information on these studied parameters, derivations and physical connotations is available in [29]. Consequently, the current study does not discuss the derivation method for these indicators. The considered sustainability parameters based on Fig. 1 are introduced, as shown in Appendix A3. The overall exergoenvironmental impact for the kth component is expressed in Eq. (22), which is the summation of the environmental impact triggered by the manufacturing stage ($\dot{Y}_k$) and the exergy destruction ($\dot{B}_{Dk}$). The relative variation of the environmental influence of the specific fuel exergy is described by Eq. (23).

$$\dot{B}_k = \dot{Y}_k + \dot{B}_{Dk} \tag{22}$$

$$r_{bk} = \frac{b_{Pk} - b_{Fk}}{b_{Fk}} \tag{23}$$

where $r_{bk}$ is the exergoenvironmental parameter, a significant pointer that reflects the capacity to reduce the component's environmental impact. Higher value of $r_b$ connotes high environmental impact of the respective component, and reducing the environmental impact of such a component is paramount. Furthermore, the exergoenvironmental factor is presented in Eq. (24) for the kth component [30].

$$f_{b,k} = \frac{\dot{Y}_k}{\dot{Y}_k + \dot{B}_{D,k}} = \frac{\dot{Y}_k}{\dot{B}_k} \tag{24}$$

where $f_{b,k}$ is the exergoenvironmental factor, a non-dimensional parameter that expresses the relationship between the environmental impact of the system component and the totality of the environmental impact linked with the k$^{th}$ component. During the manufacturing stage, the higher values of $f_b$ signifies high environmental impact while low values denote less exergy destruction and thus less environmental impact. The exergoenvironmental impact equations ($\dot{B}$), the environmental impact rate ($\dot{Y}_k$) of the k$^{th}$ component are presented in Appendix A4. The specific environmental exergy destruction impact for the kth components is depicted in Appendix A5.

#### 2.1.7. Exergoenvironmental evaluation for the refrigerant (working fluid)

The impact of the refrigerant or working fluid is not enveloped in the exergoenvironmental model of the organic Rankine cycle. Therefore, the allocation rule has been applied by Ahmadi et al. [31], where the environmental effect of the working fluid is described. The latter is achieved by assigning the exergoenvironmental impact of the working fluid to respective components of the system based on the percentage of exergy destruction of the separate components expressed as:

$$Y_k^{wf} = y_{D,k}^{*} \times Y_{wf} \tag{25}$$

where $Y_{wf}$, described the total impact of the working fluid on the environment, $y_{D,k}^{*}$ is the ratio of exergy destruction. The overall impact of the working fluid on the environment is obtained as:

$$Y_{wf} = Y_{wf}^{con} + Y_{wf}^{om} + Y_{wf}^{dec} \tag{26}$$

where $Y_{wf}^{con}$, $Y_{wf}^{om}$, *and* $Y_{wf}^{dec}$ describes the environmental impact due to the working fluid at construction, maintenance, operation and decommissioning stages, respectively. Additionally, during the operation stage, seepage of working fluid occurs, and this is measured by the following:

$$M_{wf}^{yl} = M_{wf} \times \beta \times n \tag{27}$$

where $M_{wf}^{yl}$, is the quantity of working fluid leakage (kg), $M_{wf}$ is the working fluid quantity filled during the operation stage, $\beta$ is the annual leakage proportion of fluid (%), and $n$ is the plant years. Similarly, during decommissioning, the emission of the fluid due to the discharge of non-condensate gas is evaluated by:

$$M_{wf}^{em} = \left(M_{wf} - M_{wf}^{yl}\right) \times \gamma \tag{28}$$

where: $M_{wf}^{em}$ = quantity of emitted working fluid during decommissioning (kg)

$\gamma$ = the working fluid emission ratio (%).

#### 2.1.8. Components life cycle analysis (LCA)

The effect of the kth component on the environment is defined as:

$$Y_k = \omega_k \times M_k \tag{29}$$

where $\omega_k$ is the Eco-99 coefficient of the kth system component (mPts/kg). In contrast, the impact of the kth on the environment and the overall environmental impact for the three stages, construction, operation and decommissioning, are calculated by Eqs. (30) and (31).

$$Y^{LCA} = Y_k^{con} + Y_k^{om} + Y_k^{wf} \tag{30}$$

$$Y_k = Y^{LCA} + Y_k^{wf} \tag{31}$$

### 2.2. Selection of working fluid

Working fluid (WF) selection is very critical in operating thermodynamic cycles. A WF must possess thermo-physical and chemical stability at some temperature range for the desired application. The choice and type of fluid influence the system's performance indicators, such as efficiency and environmental impact. Nevertheless, to attain a suitable thermal match, the critical temperature of the working fluid needs to be

close to that of the waste heat [32]. For this study, three different HFC refrigerants (R245fa, R1234ze and R1234yf) are selected for their critical temperatures near the heat source. The properties of these refrigerants are obtained from REFPROP 8.0 and presented in Table 1. At the same time, the T-S diagrams are depicted in Fig. 2.

### 2.3. Thermoeconomic analysis of the plant

The cost of the system is estimated using the life cycle cost LCC ($), annualised life cycle cost ALCC ($/yr), the unit cost of energy, UCOE ($/kWh) and breakeven point, BEP (yr). Shokati et al. [34] in Eq. (32) presented the relationships for these expressions.

$$LCC = \sum_{q=1}^{z} C_q; q \in \{plant\} \tag{32}$$

where $C_q$ is the cost of the plant component, $\boldsymbol{q}$. The life cycle cost of each component is related to the purchase equipment cost $Z_k$ expressed as cost per unit of time $\dot{Z}_k$ ($/s) for the k$^{th}$ component

$$\dot{Z}_k = \frac{\varphi CRFZ_k}{3600N} \tag{33}$$

where $\varphi$ is the maintenance factor, $N$ is the number of plants operating time in hours, $CRF$ is the capital recovery factor:

$$CRF = \frac{|i|1+i|^n|}{||1+i|^n - 1|} \tag{34}$$

The annualised life cycle cost ALCC ($/yr) is estimated as

$$\mathrm{ALCC} = \mathrm{LCC}\left|\frac{1 - \left|\frac{1+d}{1+i}\right|}{\left|\frac{1+d}{1+i}\right|^n}\right| \tag{35}$$

where **d** is the inflation rate, and **i** is the interest rate.

Similarly, the unit cost of electricity (UCOE), and the brake even period, BEP, is obtained.

$$\mathrm{UCOE} = \frac{\mathrm{ALCC}}{365\mathrm{E_s}} \tag{36}$$

$$\mathrm{BEP} = \frac{\mathrm{LCC}}{\mathrm{Q_{AP}} \times \mathrm{UEC_{MC}}} \tag{37}$$

$$\mathrm{E_s} = 24\mathrm{W_{Plant}} \tag{38}$$

$$\mathrm{Q_{AP}} = 365\mathrm{E_S} \tag{39}$$

where $Q_{AP}$ (kWh/yr) is the annual energy production; $UEC_{MC}$ ($/kWh) is the cost of the conventional electricity supply; $E_s$ (kWh/day) is the daily energy demand; and $W_{Plant}$ (kW) is the plant capacity. The purchase and equipment cost is shown in Table 2.

### 2.4. Performance validation

The results from this study are validated by comparing with a related theoretical basic combined power-cooling ORC cycle (BCCP) incorporated with an ejector. Using the same operating parameters, the turbine output, evaporator cooling rate, energy efficiency, and exergy efficiency were compared with the work in Rostamzadeh [7] (Table 5). The research is the closest in system configuration to the present work. The results show significant improvement using R245fa as the common refrigerant for the validation. An improvement potential (IP) was obtained in the power output of about 36.26 %, while efficiencies followed the same improvement trend with about 48.2 % IP in the evaporator cooling rate.

## 3. Results and discussion

### 3.1. Thermodynamic inputs and flow parameters for the ORCPCES

The results of the thermoeconomic, exergoenvironmental sustainability of a power-cooling ejector ORC plant are presented. The system operated with three different refrigerants R245fa, R1234yf and R1234ze. The plant operating hours for one year is 7000 h, while the lifetime operation (n) was 20 years. These parameters with the operational data were used to develop codes in EES for the ORCPCES, generating the thermodynamic flow parameters for the different working fluids presented in Table 3. The input temperatures to the turbine for all the refrigerants were taken at 359.3 K, while the highest exergy flow rate was obtained at 366.40 kW with R1234ze, followed by R245fa and R1234yf. However, the entropy changes within the working fluids were found to vary across the components. Therefore, these entropy variations across the working fluids and components must have been responsible for the decline in the exergy flow rates.

#### 3.1.2. Thermodynamic performance of the ORCPCES under operating conditions

The ORCPES performance based on the operating parameters is presented in Fig. 3. The results show that the pump work was approximately the same at 3.33, 3.142, and 3.486 kW for R245fa, R1234yf, and R1234ze. The maximum power output was obtained at 75 kW using R1234ze, while that obtained using R245fa and R1234yf was not greater than 65 kW. The evaporator cooling rate (ECR) and the power-cooling efficiency (PCE) ranged between $120.8 \leq \mathrm{ECR} \leq 153$ kW and $28.87 \leq \mathrm{PCE} \leq 34.43$ % in that order, with the highest PCE and ECR obtained using R1234ze. The exergy efficiencies $\psi$ were calculated at 25.7 % for R245fa, 28.87 % for R1234fy and 31.68 % for R1234ze at heat inputs of 636. 642 and 707 kW, respectively. The increase in the exergy efficiency is ascribed to the reduction in the denominator factor $\left(1 - \frac{T_0}{T_{Qin}}\right)\dot{Q}_{in}$ due to high $T_{Qin}$ as well as the increase in Wnet obtained with R1234ze.

#### 3.1.3. Results of exergoenvironmental and LCA analysis

The LCA method was used to compute the environmental impacts of the components. The leakage of the working fluid into the atmosphere was also considered in the analysis. The refrigerant leakage to the atmosphere was determined from Eco 99 coefficients calculated at 7300 mPts/kg, 19,654 mPts/kg, and 5335 mPts/kg for R1234ze R1234yf, and R245fa, respectively [38]. The corresponding Eco 99 coefficients for the manufacturing phase are 150 mPts/kg, 99 mPts/kg, and 99 mPts/kg for R1234z4, R1234yf, and R245fa, respectively. The filling mass of the working fluid was obtained at 5.57 kg and 5.4 kg for a 1-kW power output generated by the turbine [39]. A 10 per cent leakage was assumed in the operation phase, leaving 90 per cent of the filled refrigerants for the operation phase. Furthermore, 3% of the leakage

**Table 1**
Physical and environmental properties of selected working fluids [33].

| Substance | Chemical formular | Molecular weight | NBP°C | $T_C$ °C | $P_{C\ MPa}$ | ODP 100yr | GDP | LFL | ALT (year) |
|---|---|---|---|---|---|---|---|---|---|
| R245fa | $CF_3$-$CH_2$-$CHF_2$ | 134.05 | 15.1 | 154.1 | 3.65 | 0.0 | 1050 | None | 7.7 |
| R1234yf | $CF_3CF{=}CH_2$ | 114.04 | -29.5 | 94.7 | 3.38 | 0.0 | <1 | 6.2 | 0.029 |
| R1234ze | $CHF{=}CHCF_3$ | 114.04 | -19.0 | 109.4 | 3.64 | 0.0 | <1 | 7.6 | 0.045 |

LFL= low flammability limit, ODP = ozone depleting potential, ALT = atmospheric lifetime years, NBP= normal boiling point.

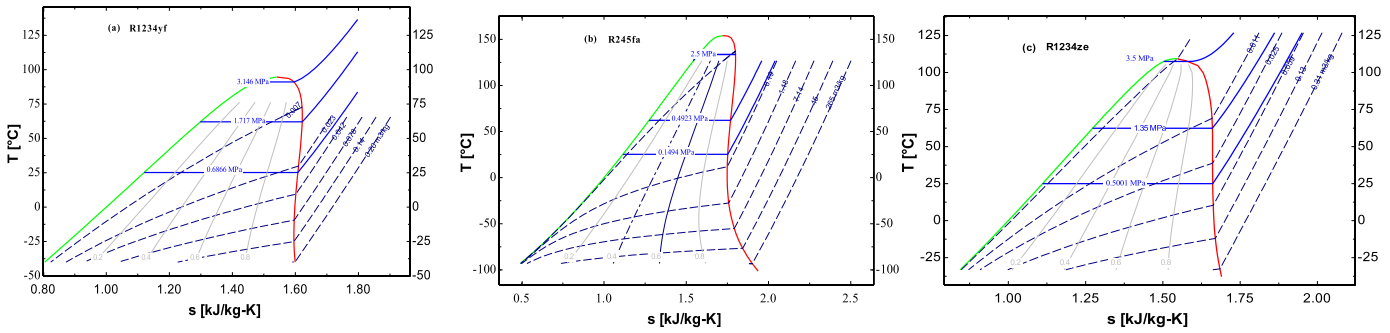


**Fig. 2.** T-s diagram for selected for working fluids (a) R245fa, (b) 1234yf and (c) R1234ze.

**Table 2**
Purchase and equipment cost for the system components [35–37].

| System component | Purchase and equipment cost function ($) |
|---|---|
| Vapour generator | $Z_{VG} = 1010\lvert A_{VG}\rvert^{0.78}$ |
| Turbine | $Z_{Turb} = \lvert \frac{479.34\dot{m}_{wf}}{0.92-\eta_{GT}} \lvert ln\rvert \frac{P_i}{P_e} \rvert \parallel 1 + exp[0.036T_i - 54.4]\rvert$ |
| Pump | $Z_{Pump} = 3540\lvert \dot{W}_P\rvert^{0.71}$ |
| Evaporator | $Z_{Evap} = 130\lvert \frac{A_{Evap}}{0.093}\rvert^{0.78}$ |
| Valve | $Z_{Valve} = 37\lvert \frac{P_i}{P_e}\rvert^{0.68}$ |
| Condenser | $Z_{Cond.} = 1773\dot{m}_{wf}$ |
| Ejector | $Z_{Ejector} = 37\lvert \frac{P_i}{P_e}\rvert^{0.68}$ |

**Table 5**
Performance validation of ORCPCES.

| Parameter | Rostamzadeh et al. [7] | Current work (ORCPCES) | Improvement potential |
|---|---|---|---|
| Turbine output (kW) | 15.64 | 24.54 | 8.9 |
| Energy efficiency (%) | 14.47 | 37.57 | 23.1 |
| Exergy efficiency (%) | 35.87 | 41.46 | 10.49 |
| Evaporator cooling rate (kW) | 17.02 | 32.87 | 15.85 |
| Refrigerant | R245fa | R245fa | - |
| Turbine inlet pressure (Bar) | 25 | 25 | - |
| Turbine inlet temperature (K) | 433 | 433 | - |
| Turbine outlet pressure (Bar) | 5.428 | 5.428 | - |
| Refrigerant mass flow rate (kg/s) | 0.5277 | 0.5277 | - |
| Intermediate pressure (corresponding to Ejector primary flow pressure) (Bar) | 1.81 | 1.81 | - |
| Flue gas inlet temperature (K) | 600 | 600 | - |
| Flue gas outlet temperature (K) | 400 | 400 | - |
| Coefficient of Performance (COP) | | | |

quantity was used for the required amount in the decommissioning phase. The corresponding values are shown for R245fa, R1234ze, and R1234yf in Fig. 4a, while the heat transfer parameters of the components are shown in Fig. 4b.

### 3.1.4. Environmental analysis of the components system in the life cycle

Table 6 depicts the environmental impact of the components in the life cycle for R245fa, R1234ze and R1234yz. The overall environmental impact due to the components was calculated at 5.1 $\times 10^5$ mPts, 5.24 $\times 10^5$ mPts and 5.4 $\times 10^5$ mPts respectively, while 4.01 $\times 10^5$ mPts 7.81 $\times 10^4$ mPts and 9.33 $\times 10^5$ mPts was due to the working fluids in that order. From the impact of the working fluid, about 18.30 % of environmental damage occurred during the decommissioning phase with R245fa. In comparison, 20.45 % and 9.86 % occurred with R1234ze and R1234yf, respectively. All the components have the same degradation coefficient because they are made from steel. The only difference exists in the quality levels. For example, the quality level for R245fa (components only) varies from 60.675 kg to 2089.776 kg. Similarly, R1234ze and R1234yf range from 65.723 to 2370.576 kg and 55.723 to 2014.584 kg, respectively. The ejector had the lowest quality while the turbine had the highest quality, followed by the vapour generator and the condenser. The variations in quality are working fluid dependant and conditions of operation. However, the largest environmental impact occurred during the operation stage.

### 3.1.5. Exergoenvironmental impact (EI) of the components

Fig. 5(a-c) shows the EI for the different refrigerants. The EI of the exergy destruction ($\dot{B}_D$) make up the total exergoenvironmental impact ($\dot{B}$). The EI values for all the system components are less than $\dot{B}_D$. Showing that the components EI are primarily composed of $\dot{B}_D$. The $\dot{B}_D$ values for R245fa, R1234yf and R1234ze range between $0.27 \leq B_D \leq 1.713$ mPts/h $0.176 \leq B_D \leq 4.02$ mPts/h and $0.285 \leq B_D \leq 3.84$ mPts/h, respectively. The $\dot{B}_D$ decreases in the order of the vapour generator, evaporator, condenser, turbine, pump and ejector. The vapour generator has the largest impact on the environment. It accounted for about 30.28 %, 35.19 % and 29.92 % of all the exergoenvironmental impact of the components using R245fa, R1234yf and R1234ze in that order while the condenser accounted for 16.18 %, 11.28 % and 13.09% for R245fa, R1234yf and R1234ze, respectively.

Figs. 6 and 7 show the difference in specific environmental $r_b$ impact and the exergeoenviromental factor $f_b$ of the components. The $r_b$ is the indicator that mirrors the capability to reduce the impact of the component on the environment. Fig. 6 indicates that the value for $r_b$ is highest in the condenser. The $r_b$ were calculated at 0.989, 0.957, and 0.898 for R245fa, R1234yf, and R1234ze, respectively. The condenser has potential for improvement, resulting from the low convective heat transfer of air used as the cooling medium and the small temperature gradient between air and the working fluid, which requires comparatively large areas for effective heat transfer. Fig. 7 depicts $f_b$ for the different components and refrigerants. The $f_b$ ranged between $0.2 \leq f_b \leq 0.99$ %, $0.04 \leq f_b \leq 0.85$ % and $0.05 \leq f_b \leq 0.96$ % for R245fa, R1234yf, and R1234ze. Also, the values of $f_b$ for the condenser, pump and turbine are the largest across the working fluids, which are higher than 30 % (0.3) of the construction value for the steel used. Therefore, it implies that the EI generated during the manufacturing stages for the components: condenser, turbine and pump constitute the highest EI. Therefore these components may be substituted with eco-friendly materials.

### 3.1.6. Sustainability indicators

The issues of sustainability are paramount to engineering systems and components. The sustainability indicators for the ORCPCES system

**Table 3**
Thermodynamic state point parameters for the working fluids.

| State | Temperature[K] | Pressure[Bar] | Enthalpy[kJ/kg] | Entropy[kJ/kg.K] | Mass[kg] | Exergy[kW] |
|---|---|---|---|---|---|---|
| R245fa | | | | | | |
| 1 | 359.3 | 1.013 | 631.50 | 6.448 | 3.40 | 364.30 |
| 2 | 353.1 | 1.013 | 424.60 | 6.048 | 3.40 | 28.64 |
| 3 | 313.6 | 18.000 | 235.50 | 1.178 | 3.0 | 28.64 |
| 4 | 346.2 | 18.000 | 487.90 | 1.811 | 3.0 | 162.30 |
| 5 | 341.0 | 7.991 | 473.20 | 1.811 | 1.20 | 47.25 |
| 6 | 328.9 | 5.434 | 452.10 | 1.771 | 2.20 | 66.49 |
| 7 | 329.2 | 4.129 | 455.90 | 1.797 | 4.00 | 104.70 |
| 8 | 313.0 | 4.129 | 252.40 | 1.178 | 1.00 | 8.48 |
| 9 | 313.0 | 4.129 | 252.40 | 1.178 | 1.00 | 8.48 |
| 10 | 313.0 | 4.129 | 252.40 | 1.178 | 3.00 | 25.43 |
| 11 | 303.6 | 1.800 | 252.40 | 1.179 | 1 | 8.11 |
| 12 | 303.6 | 1.800 | 426.80 | 1.754 | 1.00 | 10.12 |
| 13 | 333.5 | 4.129 | 460.50 | 1.811 | 1.80 | 48.11 |
| 14 | 293.0 | 1.013 | 83.30 | 0.294 | 12.97 | 0.00 |
| 15 | 305.0 | 1.013 | 146.00 | 0.503 | 12.97 | 1.19 |
| 16 | 296.0 | 1.013 | 300.40 | 5.702 | 6.68 | 0.00 |
| 17 | 274.0 | 1.013 | 274.30 | 5.611 | 6.68 | 8.02 |
| R1234yf | | | | | | |
| 1 | 359.3 | 1.013 | 631.5 | 6.448 | 3.103 | 332.7 |
| 2 | 353.1 | 1.013 | 424.6 | 6.048 | 3.103 | 62.61 |
| 3 | 297.2 | 18.000 | 232.9 | 1.114 | 3.000 | 119.2 |
| 4 | 340.1 | 18.000 | 447.0 | 1.75 | 3.000 | 188.8 |
| 5 | 339.0 | 7.211 | 426.8 | 1.750 | 1.200 | 51.38 |
| 6 | 320.1 | 12.080 | 393.1 | 1.617 | 2.200 | 108.0 |
| 7 | 323.5 | 6.500 | 407.3 | 1.698 | 4.000 | 155.4 |
| 8 | 296.4 | 6.500 | 231.9 | 1.111 | 1.000 | 39.73 |
| 9 | 296.4 | 6.500 | 231.9 | 1.111 | 1.000 | 39.73 |
| 10 | 296.4 | 6.500 | 231.9 | 1.121 | 3.000 | 119.2 |
| 11 | 257.6 | 1.800 | 231.9 | 1.126 | 1.000 | 35.07 |
| 12 | 257.6 | 1.800 | 352.7 | 1.595 | 1.000 | 15.18 |
| 13 | 334.9 | 6.500 | 424.5 | 1.750 | 1.800 | 72.90 |
| 14 | 293.0 | 1.013 | 83.30 | 0.294 | 11.180 | 0.00 |
| 15 | 308.0 | 1.013 | 146.0 | 0.5029 | 11.180 | 1.022 |
| 16 | 300.0 | 1.013 | 300.4 | 5.702 | 4.627 | 0.00 |
| 17 | 274.0 | 1.013 | 274.3 | 5.611 | 4.627 | 5.558 |
| R1234ze | | | | | | |
| 1 | 359.3 | 1.013 | 631.5 | 6.448 | 3.418 | 366.40 |
| 2 | 353.1 | 1.013 | 424.6 | 6.048 | 3.418 | 68.96 |
| 3 | 293.9 | 18.00 | 226.7 | 1.090 | 3.000 | 104.60 |
| 4 | 343.1 | 18.00 | 462.5 | 1.779 | 3.000 | 191.20 |
| 5 | 335.1 | 9.31 | 447.6 | 1.779 | 1.200 | 58.59 |
| 6 | 336.3 | 15.80 | 416.2 | 1.659 | 2.200 | 118.00 |
| 7 | 321.5 | 4.32 | 422.5 | 1.756 | 4.000 | 123.10 |
| 8 | 293.4 | 4.32 | 225.6 | 1.090 | 1.000 | 33.72 |
| 9 | 293.4 | 4.32 | 225.6 | 1.090 | 1.000 | 33.72 |
| 10 | 293.4 | 4.32 | 225.6 | 1.090 | 1.000 | 33.72 |
| 11 | 268.0 | 1.80 | 225.6 | 1.096 | 1.000 | 31.91 |
| 12 | 268.0 | 1.80 | 378.6 | 1.667 | 1.000 | 13.68 |
| 13 | 326.7 | 4.32 | 430.2 | 1.779 | 1.800 | 56.60 |
| 14 | 293.0 | 1.013 | 83.3 | 0.294 | 12.560 | 0.00 |
| 15 | 308.2 | 1.013 | 146.0 | 0.503 | 12.560 | 1.15 |
| 16 | 300.2 | 1.013 | 300.4 | 5.702 | 5.862 | 0.00 |
| 17 | 274.0 | 1.013 | 274.3 | 5.611 | 5.862 | 7.041 |

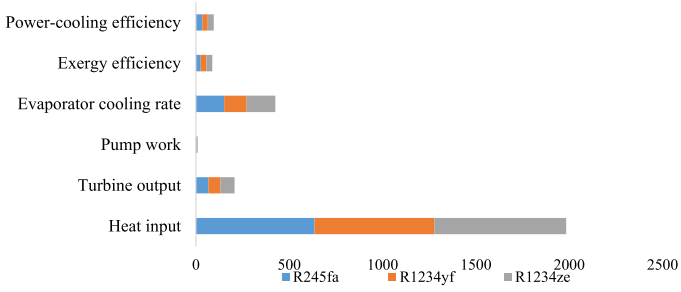


**Fig. 3.** Performance of the ORCPCES based on the operating condition.

are presented in Fig. 8, including WER, EDR, EEF and ESI. The values range between $0.302 \leq WER \leq 0.32$, $1.89 \leq EEF \leq 2.25$, $0.203 \leq EDR \leq 0.345$ and $0.455 \leq ESI \leq 0.527$ across the working fluids R245fa, R1234yf and R1234ze. However, the highest value of EEF is calculated at 2.25 and obtained using 1234yf, while the ESI of 0.526 is obtained using R1234ze. Similarly, the WER is highest using RI234yf, estimated at 0.333. Therefore, for environmental sustainability, higher values of ESI are required. The results also indicate that the total ESI for the working fluids exist at 1.43, out of which R245fa contributed about 31.95 % in promoting environmental sustainability. On the other hand, R1234yf and R1234ze contributed approximately 31.18 % and 36.89 %, respectively. Additionally, the overall EEF stood at 6.34, where R245fa caused 34.57 % of the effect on the environment, and R1234yf and R1234ze caused 35.47 % and 29.95 %.

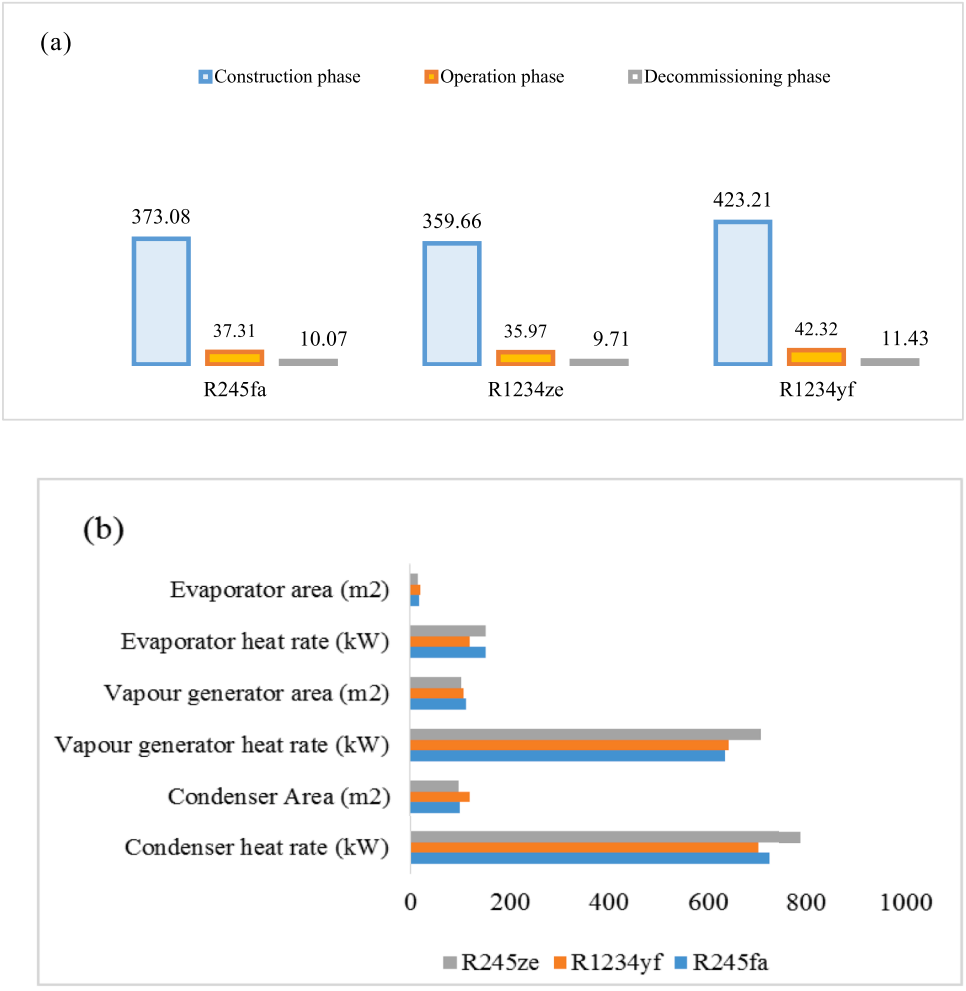


**Fig. 4.** (a) Different phases of the working fluid, (b) Heat rate and area of heat transfer components for the ORCPCES.

**Table 6**
Environmental impact of the component system on the life cycle.

| Component | Material | Degradation coefficient (mPts/kg) | Quality(kg) | $Y^{co}$(mPts) | $Y^{op}$(mPts) | $Y^{dec}$(mPts) | Y(mPts) |
|---|---|---|---|---|---|---|---|
| R245fa | | | | | | | |
| Vap. Gen | Steel | 86 | 1782.664 | 153,309.104 | 0 | 6898.90 | 160,208.01 |
| Evaporator | Steel | 86 | 266.448 | 22,914.53 | 0 | 1031.154 | 23,945.68 |
| Ejector | Steel | 86 | 60.675 | 5218.394 | 0 | 1205.023 | 6423.420 |
| Condenser | Steel | 86 | 1587.586 | 136,532.4 | 0 | 6143.958 | 142,676.4 |
| Pump | Steel | 86 | 46.648 | 4011.728 | 0 | 180.5278 | 4192.256 |
| Turbine | Steel | 86 | 2089.776 | 179,720.7 | 0 | 8087.433 | 187,808.2 |
| Fluid | R245fa | 150*/7300# | 373.0786 | 55,961.79 | 272,347.4 | 73,533.79 | 401,843 |
| R1234ze | | | | | | | |
| Vap. Gen. | Steel | 86 | 1625.65 | 139,805.9 | 0 | 6291.26 | 146,097.16 |
| Evaporator | Steel | 86 | 228.384 | 19,641.02 | 0 | 883.8461 | 20,524.87 |
| Ejector | Steel | 86 | 65.723 | 5652.178 | 0 | 1460.519 | 7112.689 |
| Condenser | Steel | 86 | 1554.28 | 133,668.1 | 0 | 6015.064 | 139,683.1 |
| Pump | Steel | 86 | 48.804 | 4197.144 | 0 | 188.8715 | 4386.015 |
| Turbine | Steel | 86 | 2370.576 | 203,869.5 | 0 | 9174.129 | 213,043.7 |
| Fluid | R1234ze | 99*/19,654# | 359.6549 | 35,605.84 | 706,865.7 | 190,853.7 | 933,325.3 |
| R1234yf | | | | | | | |
| Vap. Gen. | Steel | 86 | 1719.224 | 147,853.264 | 0 | 6653.39 | 154,506.66 |
| Evaporator | Steel | 86 | 336.232 | 28,915.95 | 0 | 1301.218 | 30,217.17 |
| Ejector | Steel | 86 | 55.723 | 4792.178 | 0 | 1238.289 | 49,159.47 |
| Condenser | Steel | 86 | 1898.442 | 163,266 | 0 | 7346.971 | 170,613 |
| Pump | Steel | 86 | 43.988 | 3782.968 | 0 | 170.2336 | 3953.202 |
| Turbine | Steel | 86 | 2014.584 | 173,254.2 | 0 | 7796.44 | 181,050.7 |
| Fluid | R1234yf | 99*/674# | 423.2086 | 41,897.65 | 28,524.26 | 7701.55 | 78,123.46 |

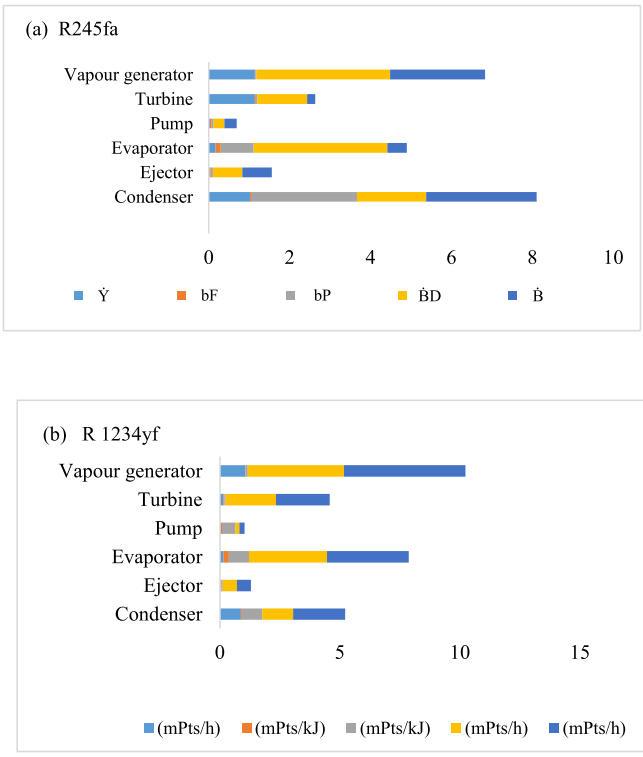


**Fig. 5.** Exergoenvironmental impact of the components with (a) R245fa, (b) R1234yf and (c) R1234ze.

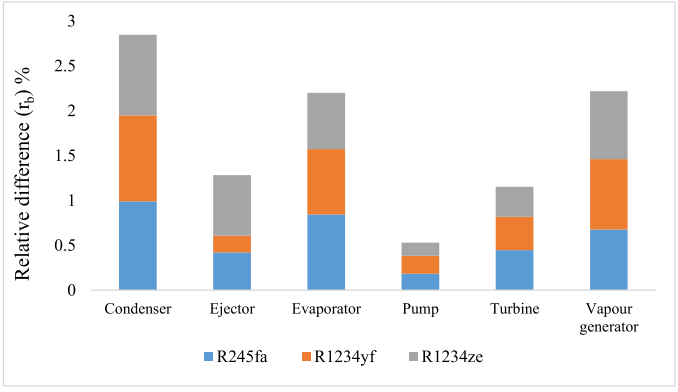


**Fig. 6.** The relative difference in specific environmental impact.

### 3.1.7. Cost analysis of the ORCPCES

The equipment cost and thermoeconomic indices for the plant are presented for the different refrigerants in Table 7. The performance is obtained with the life cycle cost LCC ($), annualised life cycle cost ALCC ($/yr), the unit cost of energy, UCOE ($/kWh) and breakeven point BEP (yr). Comparison is made with these cost indices across all the working fluids. The evaporator, vapour generator and turbine had the highest component cost. For the evaporator, the component cost was maximum at 66,943$ using R1234yf, while the turbine was minimum at 20, 925$ and 29,317$ using R1234yf and R1234ze, respectively. The least LCC, UCOE, and BEP were obtained when the system was run with R1234ze. The unit cost of electricity stood at 0.181 $/kWh with a break-even of about 22 months. The initial life cycle cost remained high for R245fa and R1234yf, with values calculated at 147,253 $ and 145,112 $, respectively.

## 4. Sensitivity analysis of the ORCPCES

Sensitivity analysis was performed on the ORCPCES system to evaluate variables that considerably influence the system's performance.

### 4.1. Effect of evaporator pressure on exergy destruction

The effect of evaporator pressure (EVPP) on exergy destruction (ED) for the different working fluids is shown in Fig. 9. The ED increases with an increase in EVPP. Maximum values of ED were obtained at EVPP of 4 bar estimated at 159 kW, 175 kW and 185 kW for R1234yf, R1234ze and R245fa, respectively. The least ED occurred with R1234yf at 1.2 bar, estimated at 108 kW. The highest ED rate was obtained with R245fa. The exergy destruction gap at EVPP of 1.2 bar between R245fa and R1234yf was calculated at 30.76 %, while R1234ze was 19.23 %. The study inferred that the evaporator pressures should be moderate at design and operation conditions since this parameter affects system performance.

#### 4.1.2. Effect of turbine back pressure and ejector mass flow rate on cooling rate

The effect of turbine back pressure (TBP) and ejector mass flow rate (EMR) on the cooling rate or refrigerating capacity is shown in Fig. 10a and 10b. From Fig. 10a, the cooling rate decreases with an increase in the TBP between 1.2 and 4 bar. The decrease in the cooling rates of the refrigerants between the TBP values was 21.84 %, 22.15 % and 23.91 % for R1234yf, R1234ze and R245fa, respectively. Similarly, the increase in EMR led to a rise in the cooling rate (Fig. 10b) by 42.91 %, 42.85 % and 42.87 % for R1234yf, R1234ze and R245fa in that order. The refrigerating capacities for R1234yf and R245fa are close, with a variance of 0.04 %. The latter is attributed to their comparable thermodynamic properties, such as critical temperatures and pressures.

#### 4.1.3. Effect of TBP on sustainability indicators

The effect of the TBP on exergetic sustainability index (ESI), waste exergy ratio (WER) and environmental effect factor (EEF) is presented in Fig. 11(a-c) for R1234yf, R1234ze and R245fa. The ESI decreases for all the refrigerants. Similarly, the WER and EEF increase with an increase in TBP. Therefore, the decrease in ESI indicates low system exergy efficiency. At the same time, an increase in WER and EEF shows that high waste is discharged into the environment. Therefore, TBP is a critical parameter affecting system performance and environmental sustainability. Nonetheless, Fig. 11 shows that at a high TBP of 4 bar, the ESI reduces between 39.95 and 50.96 % across the working fluids while WER increases steadily at all values of TBP. Maximum WER of 0.688 was obtained using R1234yf, while EEF is maximum with R245fa calculated at 0.837. Therefore, good sustainability values are obtained when the system is operated at low TBP across the working fluids.

#### 4.1.4. Effect of turbine inlet temperature (TIT) on power output and efficiency

The effect of TIT on power output and exergy efficiency (EE) is presented in Table 8. Turbine output increases from 63.66 kW to 100 kW with R1234yf. For R1234ze and R245fa, the turbine output increases

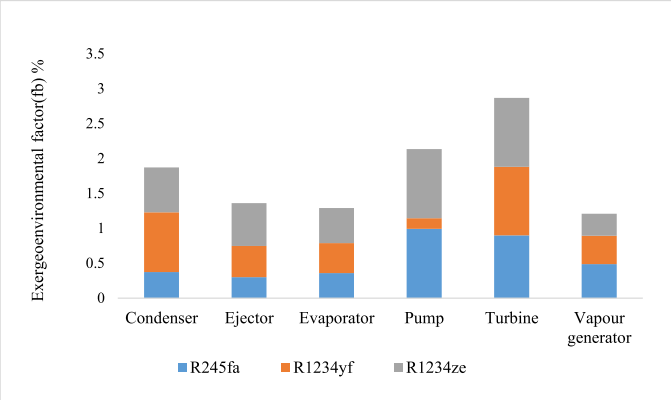


**Fig. 7.** Exergoenvironmental factor of the components.

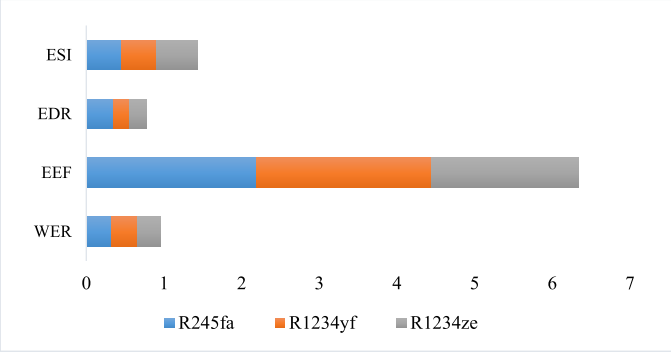


**Fig. 8.** Sustainability indicators for the ORCPCES.

**Table 7**
Equipment cost and economic indices of the ORCPCES.

| Component | Purchase of equipment cost ($) | | |
|---|---|---|---|
| | R245fa | R1234yf | R1234ze |
| Condenser | 7092 | 7092 | 7092 |
| Ejector | 5522 | 3031 | 2912 |
| Evaporator | 55,835 | 66,943 | 49,509 |
| Pump | 8321 | 7980 | 8592 |
| Turbine | 30,246 | 20,925 | 29,317 |
| Valve | 65.07 | 88.59 | 67.1 |
| Vapour generator | 40,172 | 39,052 | 37,384 |
| Thermoeconomic indices | | | |
| LCC ($) | 147,253 | 145,112 | 134,874 |
| ALCC ($/yr) | 131,519 | 129,607 | 120,463 |
| UCOE ($/kWh) | 0.2241 | 0.2291 | 0.181 |
| BEP (yr) | 2.29 | 2.341 | 1.849 |

from 77.5 to 106.9 kW and 14.8 to 91.16 kW. The TITs are different for the working fluids chosen based on their critical temperatures. The maximum exergy efficiency of 39.06 % was achieved with R1234yf at TIT of 400 K. In comparison, 36.9 % and 31.23% were obtained with R1234ze and R245fa at TIT of 405 K and 410 K, respectively. The study shows that for every degree rise in TIT, the EE increases by 0.75 % with R1234yf, whereas R1234ze and R245fa EE increases by 0.73 and 0.76 %, respectively.

*4.1.5. Effect of TBP and EMR on the unit cost of electricity*

Fig. 12a and Fig. 12b show the effect of TBP and EMR on the unit cost of electricity (UCOE). The UCOE increases with an increase in TBP for all the working fluids (Fig. 12a). The minimum UCOE occur with R245fa at 0.1287$/kW followed by R1234yf with a UCOE of 0.1427$/kW. This is ascribed to the reduction in the turbine's power output. In Fig. 12b, the

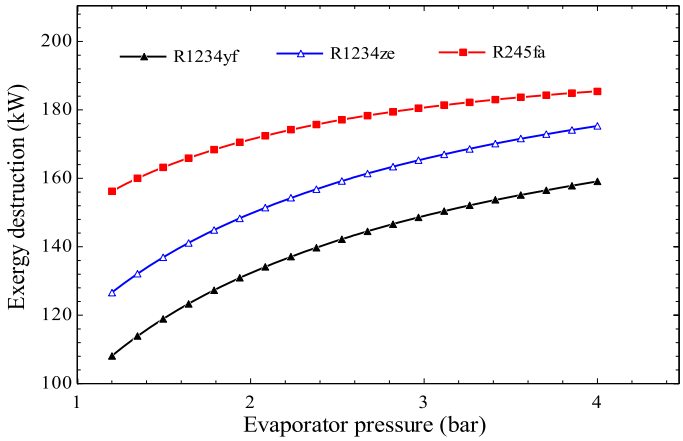


**Fig. 9.** Effect of evaporator pressure on exergy destruction for the ORCPCES.

UCOE decreases with an increase in EMR for R1234yf, R1234yz and R245fa. The least UCOE (0.1234$/kW) occur with R1234ze at an EMR of 1.75 kg/s. For increased EMR, there is a reduction in pump work and a corresponding increase in the total work output of the turbine. The increase in the total work output was responsible for the decrease in the UCOE.

## 5. Conclusion

The thermoeconomic, exergoenvironmental and sustainability analysis of a power-cooling ejector ORC plant with turbine bleeding is presented. Three organic refrigerants, R245fa, R1234yf, and R1234ze - were used for the study. In addition, the life cycle analysis was consid-

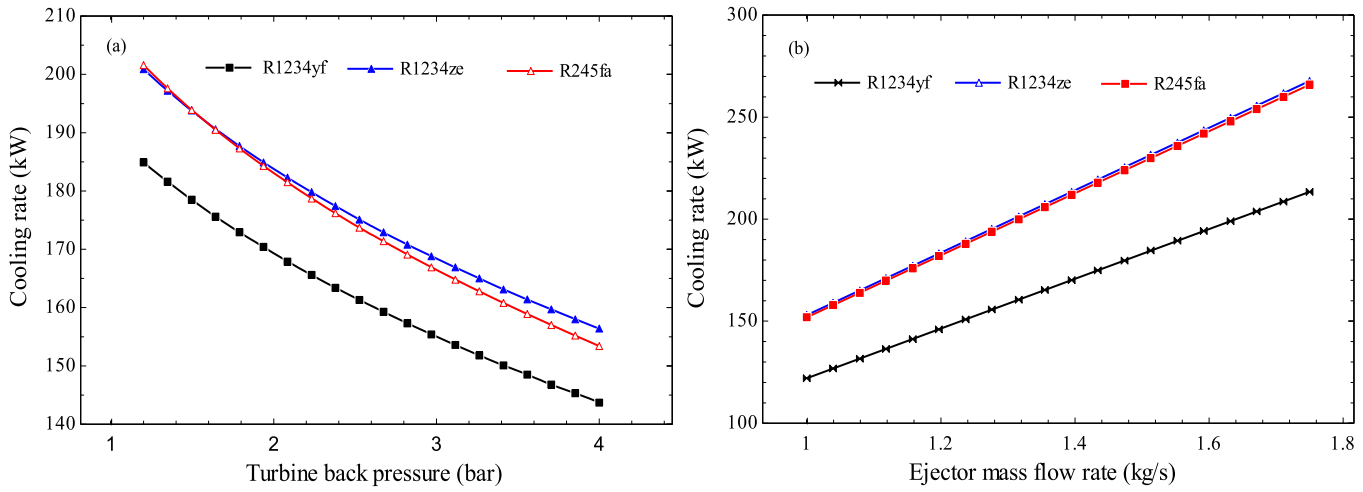


**Fig. 10.** Effect of (a) TBP and (b) EMR on ORCPCES cooling rate.

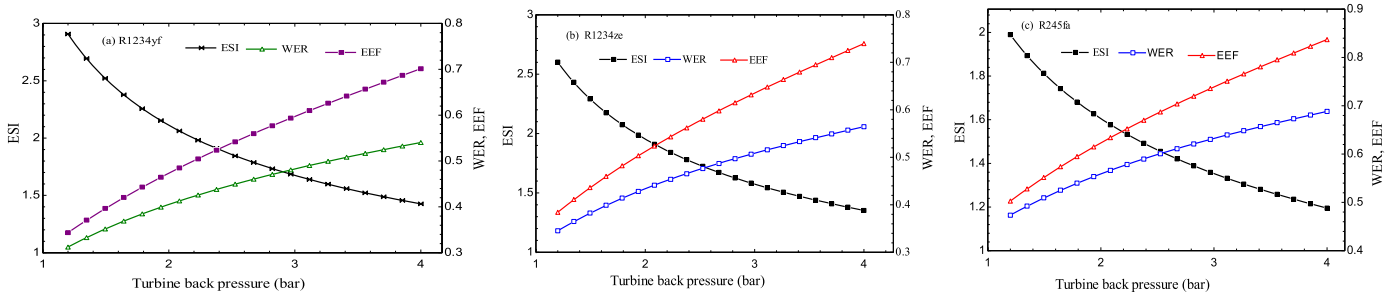


**Fig. 11.** Effect of TBP on ORCPCES on sustainability indicators with (a) R1234yf, (b) R1234ze and (c) R245fa.

**Table 8**
Effect of turbine inlet temperature on power output and exergy efficiency.

| R1234yf | | | R1234ze | | | R245fa | | |
|---|---|---|---|---|---|---|---|---|
| TIT (K) | Wt (kW) | EE (%) | TIT (K) | Wt (kW) | EE (%) | TIT (K) | Wt (kW) | EE (%) |
| 373.0 | 63.66 | 31.35 | 383.0 | 77.58 | 31.24 | 383 | 14.8 | 16.51 |
| 374.4 | 65.42 | 31.75 | 384.2 | 79.01 | 31.53 | 384.4 | 15.55 | 16.76 |
| 375.8 | 67.19 | 32.15 | 385.3 | 80.45 | 31.82 | 385.8 | 16.34 | 17.03 |
| 377.3 | 68.99 | 32.55 | 386.5 | 81.9 | 32.11 | 387.3 | 17.15 | 17.3 |
| 378.7 | 70.81 | 32.96 | 387.6 | 83.37 | 32.40 | 388.7 | 18.00 | 17.58 |
| 380.1 | 72.65 | 33.37 | 388.8 | 84.86 | 32.70 | 390.1 | 63.19 | 24.8 |
| 381.5 | 74.51 | 33.77 | 389.9 | 86.36 | 32.99 | 391.5 | 65.04 | 25.24 |
| 382.9 | 76.39 | 34.18 | 391.1 | 87.87 | 33.29 | 392.9 | 66.91 | 25.68 |
| 384.4 | 78.29 | 34.59 | 392.3 | 89.39 | 33.59 | 394.4 | 68.81 | 26.13 |
| 385.8 | 80.20 | 35.00 | 393.4 | 90.93 | 33.89 | 395.8 | 70.73 | 26.58 |
| 387.2 | 82.13 | 35.41 | 394.6 | 92.48 | 34.19 | 397.2 | 72.68 | 27.04 |
| 388.6 | 84.08 | 35.82 | 395.7 | 94.04 | 34.49 | 398.6 | 74.65 | 27.5 |
| 390.1 | 86.04 | 36.23 | 396.9 | 95.61 | 34.79 | 400.1 | 76.64 | 27.96 |
| 391.5 | 88.02 | 36.64 | 398.1 | 97.20 | 35.09 | 401.5 | 78.65 | 28.42 |
| 392.9 | 90.01 | 37.05 | 399.2 | 98.79 | 35.39 | 402.9 | 80.69 | 28.89 |
| 394.3 | 92.01 | 37.45 | 400.4 | 100.4 | 35.69 | 404.3 | 82.75 | 29.36 |
| 395.7 | 94.03 | 37.86 | 401.5 | 102.0 | 35.99 | 405.7 | 84.82 | 29.82 |
| 397.2 | 96.06 | 38.26 | 402.7 | 103.6 | 36.30 | 407.2 | 86.92 | 30.29 |
| 398.6 | 98.09 | 38.66 | 403.8 | 105.3 | 36.60 | 408.6 | 89.03 | 30.76 |
| 400.0 | 100.10 | 39.06 | 405.0 | 106.9 | 36.90 | 410.0 | 91.16 | 31.23 |

ered from the plant's construction, operation and decommissioning phases. From the study, the following deductions were arrived at: The ORC system configuration has relatively high energy and exergy efficiencies of about 34.43 %, 28.87 %, 32.28 % and energy 25.7%, 31.27% and 31.68% for R245fa, R1234yf, and R1234ze, respectively). The efficiency enhancement is due to the additional cooling provided by the ejector refrigeration system. The additional product by the ejector system was 151.9, 120.8, and 153 kW for R245fa, R1234yf, and R1234ze, respectively. Therefore, R245fa and R1234ze are thermodynamically better options for running the developed system. The total environmental effect owing to the components exists at $5.1 \times 10^5$ mPts, $5.24 \times 10^5$ mPts and $5.4 \times 10^5$ mPts for R245fa, R1234yf, and R1234ze, respectively, whereas $4.01 \times 10^5$ mPts $7.81 \times 10^4$ mPts and $9.33 \times 10^5$ mPts was due to the working fluids in that order. The least LCC, UCOE, and BEP were obtained when the system was run with R1234ze. The unit cost of electricity stood at 0.181 $/kWh with a break-

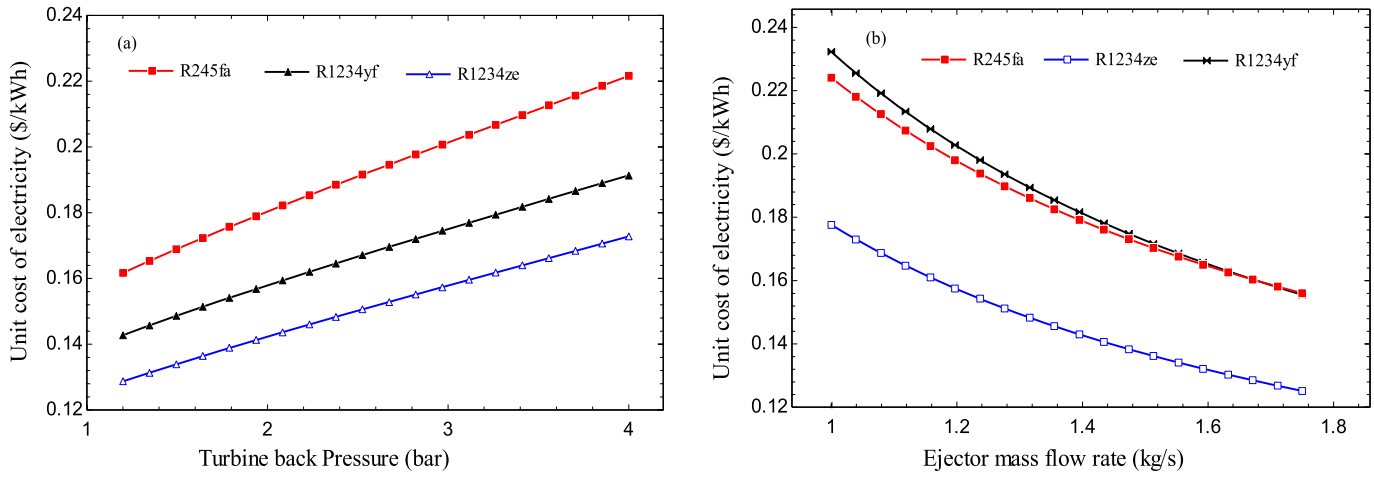


**Fig. 12.** (a) Effect of TBP on the unit cost of electricity and (b) effect of EMR on the unit cost of electricity.

even period of about one year and ten months. The sustainability parameters are better using R245fa and R1234yf. System optimisation will be necessary since the system's performance is based on working fluid and operating conditions. Alternative heat transfer fluid and refrigerants can be employed for improved system performance.

## Declaration of Competing Interest

The authors declare that there is no conflicting interest.

## Acknowledgement

The authors express their gratitude to the Africa Centre of Excellence for Sustainable Power and Energy Development, University of Nigeria Nsukka, Nigeria, for supporting this research

## Appendix A1

Process description and component energy balance

| Component | Process description | Energy balance |
|---|---|---|
| VG | Process 13–14, constant pressure heat-absorbing states by the working fluid | $Q_{vg,3-4} = \dot{m}_1 h_1 - \dot{m}_3 h_3 = \dot{m}_4 h_4 - \dot{m}_2 h_2$ |
| Turbine | Process 4–12 is the expansion process of the working fluid. | $\dot{w}_{turb} = \dot{m}_1 h_1 - \dot{m}_2 h_2 = (1 - x)(h_2 - h_3) \times \eta_{turb}$ |
| Valve | Process 9–11, throttling process: constant enthalpy. | $\dot{m}_9 h_9 = \dot{m}_{11} h_{11}$ |
| Condenser | Process 7–8 is under constant pressure, condensation processes for the working fluid | $\dot{Q}_{cond,1} = \dot{m}_7 h_7 - \dot{m}_8 h_8 = \dot{m}_{7,8}(h_4 - h_5) = \dot{m}_{15} h_{15} - \dot{m}_{14} h_{14}$ |
| Ejector | Process 5–6, under constant enthalpy | $\dot{m}_5 h_5 + \dot{m}_{12} h_{12} = \dot{m}_6 h_6$ |
| Pump | Process 10–3, the isentropic pumping process | $\dot{w}_{pump} = \dot{m}_3 h_3 - \dot{m}_{10} h_{10} = \dot{m}(h_3 - h_{10}) \times \eta_{pump}, \dot{m}_3 = \dot{m}_{11}$ |

## Appendix A2

Equations describing exergy parameters for the system

| Components | $(\dot{E}_{P,k})$ | $(\dot{E}_{F,k})$ | Exergy balance | $\dot{E}_D$ | $(\psi_k)$ |
|---|---|---|---|---|---|
| VG | $\dot{E}_4 - \dot{E}_3$ | $\dot{E}_1 - \dot{E}_2$ | $\dot{E}_1 + \dot{E}_3 + \dot{E}_D = \dot{E}_4 + \dot{E}_2$ | $\dot{E}_D = \dot{E}_4 + \dot{E}_2 - \dot{E}_1 - \dot{E}_3$ | $\frac{\dot{E}_4 - \dot{E}_3}{\dot{E}_1 - \dot{E}_2}$ |
| Turbine | $\dot{W}_t$ | $\dot{E}_4 - \dot{E}_5 - \dot{E}_{13}$ | $\dot{E}_4 + \dot{E}_D = W_T + \dot{E}_5 + \dot{E}_{13}$ | $\dot{E}_D = W_T + \dot{E}_5 + \dot{E}_{13} - \dot{E}_4$ | $\frac{\dot{W}_t}{\dot{E}_4 - \dot{E}_5 - \dot{E}_{13}}$ |
| Valve | $\dot{E}_{11}$ | $\dot{E}_9$ | $\dot{E}_9 + \dot{E}_D = \dot{E}_{11}$ | $\dot{E}_D = \dot{E}_{11} - \dot{E}_9$ | $\frac{\dot{E}_9}{\dot{E}_{11}}$ |
| Condenser | $\dot{E}_{15} - \dot{E}_{14}$ | $\dot{E}_7 - \dot{E}_8$ | $\dot{E}_7 + \dot{E}_{14} + \dot{E}_D = \dot{E}_8 + \dot{E}_{15}$ | $\dot{E}_D = \dot{E}_8 + \dot{E}_{15} - \dot{E}_7 - \dot{E}_{14}$ | $\frac{\dot{E}_{15} - \dot{E}_{14}}{\dot{E}_7 - \dot{E}_8}$ |
| Evaporator | $\dot{E}_{11} - \dot{E}_{12}$ | $\dot{E}_{16} - \dot{E}_{17}$ | $\dot{E}_{11} + \dot{E}_{16} + \dot{E}_D = \dot{E}_{12} + \dot{E}_{17}$ | $\dot{E}_D = \dot{E}_{12} + \dot{E}_{17} - \dot{E}_{11} - \dot{E}_{16}$ | $\frac{\dot{E}_{11} - \dot{E}_{12}}{\dot{E}_{16} - \dot{E}_{17}}$ |
| Ejector | $\dot{E}_6$ | $\dot{E}_5 + \dot{E}_{12}$ | $\dot{E}_5 + \dot{E}_{12} + \dot{E}_D = \dot{E}_6$ | $\dot{E}_D = \dot{E}_6 - \dot{E}_5 - \dot{E}_{12}$ | $\frac{\dot{E}_6}{\dot{E}_5 + \dot{E}_{12}}$ |
| Pump | $\dot{E}_3 - \dot{E}_{10}$ | $\dot{W}_P$ | $\dot{E}_{10} + \dot{E}_D = \dot{E}_3 + \dot{W}_P$ | $\dot{E}_D = \dot{E}_3 + \dot{W}_P - \dot{E}_{10}$ | $\frac{\dot{E}_3 - \dot{E}_{10}}{\dot{W}_P}$ |

## Appendix A3

Exergetic sustainability indicators (ESI) and their derivation

| S/N | Exergetic sustainability indicators (ESI) | Derivation of ESI |
|---|---|---|
| 1 | Waste exergy ratio (WER) =Total exergy useful output/Total exergy input | $\frac{\dot{E}_1 + \dot{D}_{Total}}{\dot{E}_1 - \dot{E}_2}$ (Ranging from 0 to 1) |
| 2 | Environmental effect factor (EEF) = Waste exergy ratio/Exergy efficiency | $\frac{\dot{E}_1 + \dot{D}_{Total}}{W_T + \dot{E}_{R,\ evp}}$ (Ranging from 0 to ∞) |
| 3 | Exergy destruction ratio (EDR) = Total exergy destruction / Total exergy input | $\frac{\dot{D}_{Total}}{\dot{E}_1 - \dot{E}_2}$ (Ranging from 0 to 1) |
| 4 | Exergetic sustainability index (ESI) = Total exergy of useful output /Total waste exergy output | $\frac{W_T + \dot{E}_{R,\ evp}}{\dot{E}_{13} + \dot{D}_{Total}}$ (Ranging from 0 to ∞) |

## Appendix A4

Exergoenvironmental impact equation for the ORCPCES components

| Component | Exergoenvironmental impact equation | Auxiliary equation |
|---|---|---|
| Vapour generator | $\dot{B}_1 + \dot{B}_3 + \dot{Y}_{vg} = \dot{B}_{2+}\dot{B}_4, \dot{Y}_{vg} = \frac{Y_{vg}}{(\tau \times n)}$ | $\frac{\dot{B}_1}{\dot{E}_1} = \frac{\dot{B}_2}{\dot{E}_2}$ |
| Turbine | $\dot{B}_4 + \dot{Y}_{tub} = \dot{B}_5 + \dot{B}_{13} + \dot{B}_{wt}\dot{Y}_{tub} = \frac{Y_{tub}}{(\tau \times n)}$ | $\frac{\dot{B}_4}{\dot{E}_4} = \frac{\dot{B}_5}{\dot{E}_5}, \frac{\dot{B}_5}{\dot{E}_5} = \frac{\dot{B}_{14}}{\dot{E}_{13}}$ |
| Valve | $\dot{B}_9 + \dot{Y}_{val,} = \dot{B}_{11}, \dot{Y}_{val} = \frac{Y_{val}}{(\tau \times n)}$ | $\frac{\dot{B}_9}{\dot{E}_9} = \frac{\dot{B}_{11}}{\dot{E}_{11}}$ |
| Condenser | $\dot{B}_7 + \dot{B}_{14} + \dot{Y}_{con} = \dot{B}_8 + \dot{B}_{15,}\ \dot{Y}_{con} = \frac{Y_{con}}{(\tau \times n)}$ | $\frac{\dot{B}_7}{\dot{E}_7} = \frac{\dot{B}_8}{\dot{E}_8}$ |
| Evaporator | $\dot{B}_{11} + \dot{B}_{16} + \dot{Y}_{evp} = \dot{B}_{12} + \dot{B}_{17,}\dot{Y}_{evp} = \frac{Y_{evp}}{(\tau \times n)}$ | $\frac{\dot{B}_{16}}{\dot{E}_{16}} = \frac{\dot{B}_{17}}{\dot{E}_{17}}$ |
| Ejector | $\dot{B}_5 + \dot{B}_{12} + \dot{Y}_{EJCT} = \dot{B}_6, \dot{Y}_{Eje} = \frac{Y_{EJCT}}{(\tau \times n)}$ | $\frac{\dot{B}_5}{\dot{E}_5} = \frac{\dot{B}_6}{\dot{E}_6}, \frac{\dot{B}_5}{\dot{E}_5} = \frac{\dot{B}_{12}}{\dot{E}_{12}}$ |
| Pump | $\dot{B}_{10} + \dot{Y}_{pum} + \dot{B}_{wp} = \dot{B}_3, \dot{Y}_{pum} = \frac{Y_{pum}}{(\tau \times n)}$ | $\frac{\dot{B}_{10}}{\dot{E}_{10}} = \frac{\dot{B}_3}{\dot{E}_3}$ |

## Appendix A5

Specific environmental and exergy destruction impact for the kth components

| Component | Fuel | Product | Exergy destruction |
|---|---|---|---|
| Vapour generator | $b_{F,VG} = \frac{b_1 \times E_1 - b_2 \times E_2}{E_1 - E_2}$ | $b_{P,VG} = \frac{b_4 \times E_4 - b_3 \times E_3}{E_4 - E_3}$ | $B_{D,VG} = b_{F,VG} \times \dot{E}_{D,VG}$ |
| Turbine | $b_{F,\ turb} = \frac{b_4 \times \dot{E}_4 - b_5 \times \dot{E}_5 - b_{13} \times \dot{E}_{13}}{\dot{E}_4 - \dot{E}_5 - \dot{E}_{13}}$ | $b_{P,turb} = b\dot{w}_t$ | $B_{D,turb} = b_{F,turb} \times \dot{E}_{D,turb}$ |
| Valve | | | |
| Condenser | $b_{F,\ cond} = \frac{b_7 \times \dot{E}_7 - b_8 \times \dot{E}_8}{\dot{E}_7 - \dot{E}_8}$ | $b_{P,cond} = \frac{b_{15} \times \dot{E}_{15} - b_{14} \times \dot{E}_{14}}{\dot{E}_{15} - \dot{E}_{14}}$ | $B_{D,cond} = b_{F,cond} \times \dot{E}_{D,cond}$ |
| Evaporator | $b_{F,\ evap} = \frac{b_{16} \times \dot{E}_{16} - b_{17} \times \dot{E}_{17}}{\dot{E}_{16} - \dot{E}_{17}}$ | $b_{P,evp} = \frac{b_{12} \times \dot{E}_{12} - b_{11} \times \dot{E}_{11}}{\dot{E}_{12} - \dot{E}_{11}}$ | $B_{D,evap} = b_{F,evap} \times \dot{E}_{D,evap}$ |
| Ejector | $b_{F,\ Eje} = \frac{b_5 \times \dot{E}_5 + b_{12} \times \dot{E}_{12} - b_6 \times \dot{E}_6}{\dot{E}_5 - \dot{E}_6}$ | $b_{P,\ Eje} = \frac{b_6 \times \dot{E}_6}{\dot{E}_6}$ | $B_{D,eje} = b_{F,eje} \times \dot{E}_{D,eje}$ |
| Pump | $b_{F,\ Pump} = b \times Wp$ | $b_{P,pump} = \frac{b_3 \times \dot{E}_3 - b_{10} \times \dot{E}_{10}}{\dot{E}_3 - \dot{E}_{10}}$ | $B_{D,pump} = b_{F,pump} \times \dot{E}_{D,pump}$ |

## References


[1] CN Markides, The role of pumped and waste heat technologies in a high efficiency sustainable energy future for the UK, Appl. Thermal Eng. 53 (2) (2013) 197–209.

[2] PV Elumalai, RK Moorthy, M Parthasarathy, HI Owamah, CA Saleel, CC Enweremadu, MS Reddy, A Afzal, Artificial neural networks model for predicting the behavior of different injection pressure characteristics powered by blend of biofuel- nanoemulsion, Energy Sci. Eng. 10 (2022) 2367–2396.

[3] P Haghparast, MV Sorin, MA Richard, H Nesreddine, Analysis and design optimisation of an ejector integrated into an organic Rankine cycle, Appl. Therm. Eng. 159 (2019), 113979.

[4] G Pei, J Li, Y Li, D Wang, J Ji, Construction and dynamic test of a small-organic Rankine cycle, Energy 36 (2011) 3215–3223.

[5] SU Wenqiang, Y Xiaoyu, W Yanhui, Exergy efficiency analysis of ORC (Organic Rankine Cycle) and ORC based combined cycles driven by low-temperature waste heat, Energy Convers. Manage. 135 (2017) 63–73.
[6] K Zhang, X Chen, CN Markides, Y Yang, S Shen, Evaluation of ejector performance in an organic Rankine cycle, Appl. Energy 184 (2016) 404–412.
[7] H Rostamzadeh, M Ebadollahi, H Ghaebi, M Amidpour, R Kheiri, Energy and exergy analysis of novel combined cooling and power (CCP) cycles, Appl. Therm. Eng. (2017), https://doi.org/10.1016/j.applthermaleng.2017.06.011.
[8] R Kheiri, H Ghaebi, M Ebadollahi, H Rostamzadeh, and Thermodynamic modeling and Performance analysis of four new integrated organic Rankine cycles (A comparative study), Appl. Therm. Eng. (2017), https://doi.org/10.1016/j.applthermaleng.2017.04.150.
[9] M Ebadollahi, H Rostamzadeh, H Ghaebi, M Amidpour, Exergoeconomic analysis and optimisation of innovative cascade bi-evaporator electricity/cooling cycles with two adjustable cooling temperatures, Appl. Therm. Eng. 152 (2019) 890–906, https://doi.org/10.1016/j.applthermaleng.2019.02.110.
[10] B Zheng, YW Weng, A combined power and ejector refrigeration cycle for low temperature heat sources, Sol. Energy 84 (2010) 784–791.
[11] Y Zhu, W Li, Y Wang, H Li, S Li, Thermodynamic analysis and parametric optimisation of ejector heat pump integrated with organic Rankine cycle combined cooling, heating and power system using zeotropic mixtures, Appl. Therm. Eng. 194 (2021), 117097.
[12] JCS Garcia, MS Berana, Thermodynamic analysis and performance evaluation of a proposed novel combined cooling and power system, Philippine Eng. J. PEJ 41 (1) (2020) 1–18.
[13] A Habibzadeh, MM Rashidi, N Galanis, Analysis of a combined power and ejector-refrigeration cycle using low temperature heat, Energy Convers. Manage. 65 (2013) 381–391.
[14] N Toujani, N Bouaziz, M Chrigui, L Kairouani. Performance analysis of a new combined organic Rankine cycle and vapor compression cycle for power and refrigeration cogeneration. Pr. Inst. Masz. Przeplyw., Pol. Akad. Nauk, 140 (2018) 39–81.
[15] W Gu, YW Weng, SL Weng, GY Cao, The latest research findings concerning low-temperature heat energy-based power generation and its development trend, J. Eng. Them. Energy Power 22 (2) (2007) 115–122.
[16] Z Hajabdollahi, F Hajabdollah, M Tehran, H Hajabdollahi, Thermo-economic environmental optimisation of Organic Rankine cycle for diesel waste heat recovery, Energy 63 (2013) 1425–1435.
[17] MHD Hettiarachchi, M Golubovic, WM Worek, Y Ikegami, Optimum design criteria for an organic Rankine cycle using low-temperature geothermal heat sources, Energy 32 (2007) 1698–1706.
[18] B Saleh, G Koglbauer, M Wedland, J Fischer, Working fluids for low-temperature organic Rankine cycles, Energy 32 (2007) 1210–1221.
[19] FI Abam, EB Ekwe, SO Effiom, MC Ndukwu, TA Briggs, CH Kadurumba, Optimum exergetic performance parameters and thermo-sustainability indicators of low temperature modified organic Rankine cycles (ORCs), Sustain. Energy Technol. Assessments 30 (2018) 91–104.
[20] G Manente, A Lazzaretto, E Bonamico, Design guidelines for the choice between single and dual pressure layouts in organic Rankine cycle (ORC) systems, Energy 123 (2017) 413–431.
[21] W Yu, Y Xu, H Wang, Z Ge, J Wang, D Zhu, Y Xia, Thermodynamic and thermoeconomic performance analyses and optimisation of a novel power and cooling cogeneration system fuelled by low-grade waste heat, Appl. Therm. Eng. (2020), https://doi.org/10.1016/j.applthermaleng.2020.115667.
[22] M Wang, Y Chen, Q Liu, Z Yuanyuan, Thermodynamic and thermoeconomic analysis of dual-pressure and single pressure evaporation organic Rankine cycles, Energy Convers. Manage. 177 (2018) 718–736.
[23] S Mondal, S De, Ejector based organic flash combined power and refrigeration cycle (EBOFCP&RC) - A scheme for low grade waste heat recovery, Energy 134 (2017) 638–648.
[24] P Haghparast, MV Sorin, MA Richard, H Nesreddine, Analysis and design optimisation of an ejector integrated into an organic Rankine cycle, Appl. Therm. Eng. 159 (2019), 113979.
[25] P Ifaei, A Ataei, C Yoo, Thermoeconomic and environmental analyses of a low water consumption combined steam power plant and refrigeration Chillers-Part 2: thermoeconomic an environmental analysis, Energy Convers. Manage. (2016), https://doi.org/10.1016/j.enconman.2016.06.030.
[26] FI Abam, TA Briggs, OE Diemuodeke, EB Ekwe, KN Ujoatuonu, J Isaac, MC Ndukwu, Thermodynamic and economic analysis of Kalina system with integrated lithium-bromide-absorption cycle for power and cooling, Energy Rep. 6 (2020) 1992–2005.
[27] D Roy, R Ghosh, Energy and exergy analyses of an integrated biomass gasification combined cycle employing solid oxide fuel cell and organic Rankine cycle, Clean Techn. Environ. Policy (2017), https://doi.org/10.1007/s10098-017-1358-5.
[28] L Cao, J Wang, H Wang, P Zhao, Y Dai, Thermodynamic analysis of a Kalina-based combined cooling and power cycle driven by low-grade heat source, Appl. Therm. Eng. 111 (2017) 8–19.
[29] Z Fergani, D Touil, T Morosuk, Multi-criteria exergy-based optimisation of an Organic Rankine Cycle for waste heat recovery in the cement industry, Energy Convers. Manage. 112 (2016) 81–90.
[30] L Meyer, G Tsatsaronis, J Buchgeister, L Schebek, Exergoenvironmental analysis for evaluation of the environmental impact of energy conversion systems, Energy 34 (1) (2009) 75–89.
[31] P Ahmadi, I Dincer, MA Rosen, Exergo-environmental analysis of an integrated organic Rankine cycle for trigeneration, Energy Convers. Manage. 64 (2012) 447–453.
[32] H Kucuk, A Midilli, Assessment of exergetic sustainability indicators for a single layer solar drying system, Int. J. Exergy 16 (3) (2015) 278–292.
[33] B Saleh, Parametric and working fluid analysis of a combined organic Rankine vapor compression refrigeration system activated by low-grade thermal energy, J. Adv. Res. 7 (2016) 651–660.
[34] N Shokati, F Mohammadkhani, M Yari, SM Mohmoudi, MA Rosen, A comparative exergoeconomic analysis of waste heat recovery from a gas turbine modular helium reactor using organic rankine cycles, J. Sustain. 6 (1) (2014) 2474–2489.
[35] A Chitsaz, AS Mehr, SM Mahmoudi, Exergoeconomic analysis of a trigeneration system driven by a solid oxide fuel cell, Energy Convers. Manage. 106 (2015) 921–931.
[36] L Khani, SM Mohammad, A Chitsaz, AR Marc, Energy and exergoeconomic evaluation of a new power/cooling cogeneration system based on a solid oxide fuel cell, Energy 94 (2016) 64–77.
[37] SO Oyedepo, RO Fagbenle, SA Samuel, MA Mahbub, Thermoeconomic and thermoenvironomic modeling and analysis of selected gas turbine power plants in Nigeria. Energy Science and Engineering, Society of Chemical Industry and John Wiley and Sons Ltd. (2015).
[38] M Goedkoop, S Effting, M Collignon, The Eco-indicator 99: A damage-Oriented Method For Life-Cycle Impact assessment: Manual for Designers, PRé Consultants, 2000.
[39] L Bai, Life Cycle Assessment of Electricity Generation from Low Temperature Waste heat: the Influence of Working Fluid: NTNU-Norwegian University of Science & Technology, 20.

**Fidelis I. Abam**, received his PhD degree in Energy and Power Engineering from University of Nigeria Nsukka in 2011. He is currently a senior research academic with Michael Okpara University of Agriculture Umudike (MOUAU), Nigeria. Additionally, he is the head of the Energy, Exergy and Environment Research Group in Mechanical Engineering Department MOUAU. His-area of interest include Exergy, renewable energy system, multi-generation and environmental sustainability.

**Bassey B. Okon**, Holds a PhD degree in Mechanical Engineering, from University of Manchester United Kingdom in 2013. He is a senior lecturer in the Department of Mechanical Engineering, Akwa Ibom State University Ikot Akpaden, Nigeria. His-area of research include industrial system development, renewable energy systems, a building services engineering and sustainability.

**Ekwe Bassey Ekwe**, Holds a PhD degree in Mechanical Engineering, from Michael Okpara University of Agriculture Umudike in 2021. Currently he is with center for climate Change, Alex Ekueme Federal University Abakaliki, Nigeria as a Post doctorate Research Fellow.

**John Isaac** is a PhD student at the Michael Okpara University of Agriculture Umudike. He received a Master degree in Engineering from the same University in 2021.

**Samuel Oliver Effiom**, Holds a master degree from university of Cranfield and a PhD degree in Mechanical Engineering, from Michael Okpara University of Agriculture Umudike. He is a senior lecturer in the Department of Mechanical Engineering, Cross River University of Technology Calabar, Nigeria. His-research interest include, Gas turbine power system, Renewable energy systems and multi-generation plants.

**Macmanus. C. Ndukwu**, Holds a PhD degree in Agricultural and Bioresources Engineering in 2014, from Federal University of Technology Akure, Nigeria. His-is an associate Professor with Agricultural and Bioresources Department, Michael Okpara, University of Agriculture Umudike, Nigeria.

**Oliver I. Inah**, is a PhD student at the Michael Okpara University of Agriculture Umudike. He received a Master in Engineering from the same University.Currently he works as an academic researcher with Cross River University of Technology Calabar, Nigeria.

**Paschal Ateb Ubi**, B.Eng Mechanical Engineering and M.Eng in Industrial and Production Engineering. Currently He is currently working as an academic researcher in the Department of Mechanical Engineering, University of Calabar, Calabar, Nigeria.

**Prof Sunday Oyedepo**, has a PhD in Mechanical Engineering his research specifics include: Energy, Energy conservation and management, power plant optimization, and Sustainable Energy Development. He is currently a research Professor with the covenant University Ota, Nigeria.

**Prof Olayinka Ohunakin**, has a PhD in Mechanical Engineering his research specifics include: Energy, Renewable energy system, Climate change and Energy conversion and management. He is currently a research Professor with the covenant University Ota.